JAERI-Research
97-029

NUMERICAL PREDICTION OF LOCAL TRANSITIONAL FEATURES OF TURBULENT FORCED GAS FLOWS IN CIRCULAR TUBES WITH STRONG HEATING

March 1997

Koichiro EZATO,※ A.Mohsen SHEHATA,* Tomoaki KUNUGI
and Donald M.McELIGOT**

日本原子力研究所
Japan Atomic Energy Research Institute

本レポートは，日本原子力研究所が不定期に公刊している研究報告書です。
入手の問合わせは，日本原子力研究所研究情報部研究情報課（〒319-11 茨城県那珂郡東海村）あて，お申し越しください。なお，このほかに財団法人原子力弘済会資料センター（〒319-11 茨城県那珂郡東海村日本原子力研究所内）で複写による実費頒布をおこなっております。

This report is issued irregularly.
Inquiries about availability of the reports should be addressed to Research Information Division, Department of Intellectual Resources, Japan Atomic Energy Research Institute, Tokai-mura, Naka-gun, Ibaraki-ken 319-11, Japan.

編集兼発行　日本原子力研究所
印　　刷　㈱原子力資料サービス

Numerical Prediction of Local Transitional Features of Turbulent Forced Gas Flows in Circular Tubes with Strong Heating

Koichiro EZATO*, A. Mohsen SHEHATA*, Tomoaki KUNUGI and Donald M. McELIGOT**

Department of Reactor Engineering
Tokai Research Establishment
Japan Atomic Energy Research Institute
Tokai-mura, Naka-gun, Ibaraki-ken, Japan

(Received February 28, 1997)

Previous numerical simulation for the laminarization due to heating of the turbulent flow in pipe were assessed by comparison with only macroscopic characteristics such as heat transfer coefficient and pressure drop, since no experimental data on the local distributions of the velocity and temperature in such flow situation was available. Recently, Shehata and McEligot reported the first measurements of local distributions of velocity and temperature for turbulent forced air flow in a vertical circular tube with strongly heating. They carried out the experiments in three situations from turbulent flow to laminarizing flow according to the heating rate. In the present study, we analyzed numerically the local transitional features of turbulent flow evolving laminarizing due to strong heating in their experiments by using the advanced low-Re two-equation turbulence model. As the result, we successfully predicted the local distributions of velocity and temperature as well as macroscopic characteristics in three turbulent flow conditions. By the present study, a numerical procedure has been established to predict the local characteristics such as velocity distribution of the turbulent flow with large thermal-property variation and laminarizing flow due to strong heating with enough accuracy.

※ Student of Research Fellow: Kyushu University
* Xerox Corporation
** Idaho National Engineering and Environmental Laboratory

Keywords: Forced Convection, Numerical Prediction, Gas Flow, Strong Heating, Transitional Feature, Turbulence, Laminarization, Wall Heat Transfer Parameter, Pressure Drop

強加熱を受ける円管内ガス流の局所乱流遷移特性の数値予測

日本原子力研究所東海研究所原子炉研究所伝熱流動研究室
江里幸一郎*・A. Mohsen Shehata*・功力　資彰
Donald M. McEligot**

（1997年2月28日受理）

従来の管内流加熱層流化の解析は，流路内の速度場及び温度場の局所分布に関する実験結果が得られていなかったため，熱伝達係数や圧力損失等のマクロ特性量との比較のみで議論されてきた。近年，Shehata and McEligot は強加熱を受ける鉛直円管内空気流について，加熱条件に応じて乱流から層流化が発生するまでの3条件で実験を行い，管内の局所的な速度及び温度分布を初めて報告した。本研究では，この実験で得られた乱流の加熱層流化に伴う局所特性量の変化について，高精度な低レイノルズ数型2方程式乱流モデルを用いた数値解析を行い，上記実験条件に対するマクロ特性量のみならず速度及び温度分布の良好な一致を得ることに成功した。本研究により，大きな熱物性変化を伴う乱流や層流化現象を速度分布等の局所量を含め高精度に予測できる解析手法を確立することができた。

東海研究所：〒319－11　茨城県那珂郡東海村白方白根2－4
※　特別研究生：九州大学
＊　Xerox Corporation
＊＊アイダホ国立工学・環境研究所

Contents

目　　次

1 Introduction

Gas cooling offers the advantages of inherent safety, environmental acceptability, chemical inertness, high thermal efficiency and a high temperature working fluid for electrical energy generation and process heating. Consequently, helium and other gas systems are considered as coolants for advanced power reactors, both fission and fusion. To advance technology for gas-cooled reactors, the High Temperature Engineering Test Reactor (HTTR)[1] is under construction at the Oarai Research Establishment of the Japan Atomic Energy Research Institute. Concepts for fusion power plants with helium coolants include ARIES-I and ARIES-IV[2][3], DEMO[4] and Prometheus[5] in the United States and SSTR-2[6] and DREAM-2[7][8]in Japan.

These applications have in common turbulent flow with significant gas temperature variation along and/or across the cooling channels. The temperature range causes variation of the gas properties, invalidating the use of design relations such as the popular Dittus-Boelter correlation[9]. An alternative approach is to apply computational thermal fluid dynamics (CTFD) using a turbulence model that provides reasonable predictions in such flow fields[10]. Unfortunately, many proposed models provide poor predictions for convective heat transfer for forced flow in simple circular tubes even when the properties can be idealized as constant[11]; property variation and/or possible buoyancy forces increase the difficulty.

General effects of strong heating of a gas are variation of the transport properties, reduction of density causing acceleration of the flow in the central core, and - in some cases - significant buoyancy forces. Growth of the internal thermal boundary layer leads to readjustment of any previously fully-developed turbulent momentum profile. No truly fully-established conditions are reached because the temperature rises – leading, in turn, to continuous axial and radial variation of properties such as the gas viscosity.

In an application such as the HTTR (or reduction of flow scenarios in other plants) another complication arises. To obtain high outlet temperatures, design gas flow rates are kept relatively low. For example, at the exit of the HTTR cooling channels, the Reynolds number is about 3500. In this range the heat transfer parameters may appear to correspond to turbulent flow or to laminar flow or to an intermediate behavior, depending on the heating rate[12], with consequent differences in their magnitudes. The situation

where laminar values are measured at Reynolds numbers typifying turbulent flow is called "laminarization" by some authors[13]. Several authors have developed approximate criteria for the transitions between these regimes as shown in Fig. 1[14][15][16][17][18][19]. If the designer is to have confidence in a CTFD code, its turbulence model must demonstrate the "right" predictions in these conditions. The ultimate goal of the present study is to reach that state.

Most popular turbulence models have been developed for conditions approximating the constant properties idealization. Thus, before the application to gas-cooled components with high heat fluxes, they must be verified by comparison to careful measurements of the heat transfer, pressure drop and mean velocity and thermal fields with significant gas property variation.

Previous work

By comparison to the thermal entry measurements of Perkins and Worsoe-Schmidt[20], of McEligot, Magee and Leppert[21] and of Petukhov, Kirillov and Maidanik[22], Bankston and McEligot[23] were able to examine the applicability of eleven simple turbulence models to high-Reynolds-number turbulent gas flows with properties varying strongly in both axial and radial directions. Best agreement was found with a van Driest mixing length model[24] with the exponential term evaluated with wall properties. To accommodate low-Reynolds-number turbulent and laminarizing flows, McEligot and Bankston[25] modified this model further. This modification was developed by comparison to integral quantities, such as the local Stanton number, since internal profile measurements were not available for guidance.

The first investigator to succeed in applying an "advanced" turbulence model to laminarization by heating was Kawamura[26][27]. He tested predictabilities of low-Reynolds-number turbulence models, k-kL, k-ε,k-W and modified k-kL, by comparison to the heat transfer coefficients measured by Perkins and Worsoe-Schmidt[20], Coon[15], Coon and Perkins[16] and Bankston[12]. Kawamura concluded that the modified k-kL model gave good agreement with the experiments. Ogawa and Kawamura[28][29] also observed that the k-kL model predicted their local friction factor data well during laminarization.

Extending the work of Kawamura, Fujii et al.[30][31] employed three types of turbulence models, k-ε, k-ε-$\overline{uv}$ and k-kL-$\overline{uv}$, for comparisons to their measurements of strongly-heated turbulent gas flow in an annulus; they preferred the predictions seen with the latter

model. However, to date predictions from this code have not been published for flow in a circular tube.

Torii et al.[32][33] modified a k-ε model originally developed by Nagano, Hishida and Asano[34][35] and found that it compared favorably with the k-kL model for predicting the streamwise variation of the heat transfer coefficient in laminarizing flows in circular tubes. Torii et al.[36] then compared predictions from this model to their wall measurements for an annulus with the inner wall and with both walls heated; agreement was good at low and high heating rates but not at intermediate values (their $q^+ \approx 0.0031$). Torii et al.[37] also attempted to apply the Reynolds-stress model of Launder and Shima[38] to Bankston's St{Re} data for a circular tube. They concluded that the adopted model can generally reproduce the streamwise variation of laminarizing flows, but again predictive accuracy is comparatively poor in the subtle range of turbulent-to-laminar transition.

Objectives and Approach

All of the aforementioned turbulence models for strongly heated gas flow were developed without the benefit of internal velocity and temperature distributions in dominant forced flow for guidance or testing. Thus, it is not certain whether their agreements with wall data were fortuitous or not when such agreement occurred. For dominant forced convection with *significant gas property variation*, in low Mach number flow of common gases through a circular tube, the only published profile data available to guide (or test) the development of predictive turbulence models have been K. R. Perkins's measurements of mean temperature distributions[13]. Shehata obtained the first mean velocity distributions for this situation. His careful measurements are now available[39][40] to examine this problem and these serve as the bases for evaluation of the predictive technique employed in the present work. Shehata's experiment concentrated on three characteristic cases with gas property variation: turbulent, laminarizing and intermediate or "subturbulent" (as denoted by Perkins).

Recently Abe, Kondoh and Nagano[41][42] improved the turbulence model of Nagano and Tagawa[43] which, in turn, was an improvement over the model of Nagano and Hishida employed by Torii et al. The new version (AKN) can be considered "more universal" as it has been developed to treat separated flows as well as flows with pressure gradients; for this reason the principal change is use of the Kolomogorov velocity scale instead of

the friction velocity to account for near-wall and low-Reynolds-number effects. Model constants in the transport equations for turbulent kinetic energy and its dissipation rate were also reevaluated for improvement of overall accuracy.

The **objectives** of the present study are (1) to extend the AKN model to treat strongly-heated gas flows in circular tubes and (2) to examine the validity of that extension by comparison to careful measurements for the same conditions. The major new contribution is the use of internal velocity profiles, in addition to internal temperature profiles and integral parameters, in the validation for the air flow with strongly varying fluid properties.

In the following, we first describe the numerical technique and the model used for the predictions. Since the AKN model was developed for flows in wide rectangular ducts, the predictions are first verified by comparison to accepted correlations and thermal entry measurements for low-Reynolds-number flows in circular tubes under the constant properties idealization. After a brief description of Shehata's experiment, the predicted effects and trends induced by heating at the experimental conditions are examined in terms of key turbulence quantities. Then the predicted mean velocity and temperature distributions are compared to the measurements for verification. For the thermal design engineer, the main questions usually involve wall heat transfer rates and pressure drop. The predictions of these quantities are assessed with the data and we then close with a few concluding remarks.

2 Predictive Technique

2.1 Governing Equations and Numerical Procedure

In analysis of the strongly-heated gas flow with significant variation of thermal properties, it is necessary to consider their temperature-dependencies in the momentum and energy equations. However, we assume that the fluctuations of the thermal properties are sufficiently small compared with their mean values, so that we can neglect the terms including the fluctuations of the thermal properties. We deal with the steady state and axi-symmetric thermo-fluid field flowing upward in a circular tube. The working gas is taken as air in the comparisons and viscous dissipation is neglected because the Mach num-

the friction velocity to account for near-wall and low-Reynolds-number effects. Model constants in the transport equations for turbulent kinetic energy and its dissipation rate were also reevaluated for improvement of overall accuracy.

The **objectives** of the present study are (1) to extend the AKN model to treat strongly-heated gas flows in circular tubes and (2) to examine the validity of that extension by comparison to careful measurements for the same conditions. The major new contribution is the use of internal velocity profiles, in addition to internal temperature profiles and integral parameters, in the validation for the air flow with strongly varying fluid properties.

In the following, we first describe the numerical technique and the model used for the predictions. Since the AKN model was developed for flows in wide rectangular ducts, the predictions are first verified by comparison to accepted correlations and thermal entry measurements for low-Reynolds-number flows in circular tubes under the constant properties idealization. After a brief description of Shehata's experiment, the predicted effects and trends induced by heating at the experimental conditions are examined in terms of key turbulence quantities. Then the predicted mean velocity and temperature distributions are compared to the measurements for verification. For the thermal design engineer, the main questions usually involve wall heat transfer rates and pressure drop. The predictions of these quantities are assessed with the data and we then close with a few concluding remarks.

2 Predictive Technique

2.1 Governing Equations and Numerical Procedure

In analysis of the strongly-heated gas flow with significant variation of thermal properties, it is necessary to consider their temperature-dependencies in the momentum and energy equations. However, we assume that the fluctuations of the thermal properties are sufficiently small compared with their mean values, so that we can neglect the terms including the fluctuations of the thermal properties. We deal with the steady state and axi-symmetric thermo-fluid field flowing upward in a circular tube. The working gas is taken as air in the comparisons and viscous dissipation is neglected because the Mach num-

ber is small. The AKN k-ε model is employed for predicting the turbulent flow field. This model was developed for predicting separating and reattaching flows and its capabilities for channel flows at various Reynolds numbers were confirmed by the original authors.

The governing equations are as follows;

Continuity :

$$\frac{\partial}{\partial x_i}(\rho U_i) = 0 \tag{1}$$

Momentum :

$$\frac{\partial}{\partial x_j}(\rho U_j U_i) = -\frac{\partial P}{\partial x_i} + \frac{\partial}{\partial x_j}\left[\mu\left(\frac{\partial U_i}{\partial x_j} + \frac{\partial U_j}{\partial x_i}\right) - \rho\overline{u_i u_j}\right] - \rho g_i, \tag{2}$$

Energy :

$$\frac{\partial}{\partial x_j}(\rho c_p U_j T) = \frac{\partial}{\partial x_j}\left(\lambda\frac{\partial T}{\partial x_j} - \rho c_p\overline{u_j t}\right), \tag{3}$$

Turbulent kinetic energy :

$$\frac{\partial}{\partial x_j}(\rho U_j k) = \frac{\partial}{\partial x_j}\left\{\left(\mu + \frac{\mu_t}{\sigma_k}\right)\frac{\partial k}{\partial x_j}\right\} - \rho\overline{u_i u_j}\frac{\partial U_i}{\partial x_j} - \rho\varepsilon, \tag{4}$$

Dissipation rate of turbulent kinetic energy :

$$\frac{\partial}{\partial x_j}(\rho U_j \varepsilon) = \frac{\partial}{\partial x_j}\left\{\left(\mu + \frac{\mu_t}{\sigma_\varepsilon}\right)\frac{\partial \varepsilon}{\partial x_j}\right\} - \rho C_{\varepsilon 1}\frac{\varepsilon}{k}\overline{u_i u_j}\frac{\partial U_i}{\partial x_j} - \rho C_{\varepsilon 2} f_2 \frac{\varepsilon^2}{k}, \tag{5}$$

where turbulence quantities are defined as

$$-\rho\overline{u_i u_j} = \mu_t\left(\frac{\partial U_i}{\partial x_j} + \frac{\partial U_j}{\partial x_i}\right) - \frac{2}{3}\rho k\delta_{ij}, \tag{6}$$

$$\mu_t = \rho C_\mu f_\mu \frac{k^2}{\varepsilon}, \tag{7}$$

$$-\rho c_p\overline{u_j t} = \lambda_t\frac{\partial T}{\partial x_j}, \tag{8}$$

$$\lambda_t = \frac{c_p\mu_t}{\mathrm{Pr}_t}. \tag{9}$$

We consider the buoyancy effect only in the momentum equation and not in the turbulence model. Model constants and functions in equations (4), (5) and (7) are taken to be the same as in the AKN model: $C_\mu = 0.09$, $C_{\varepsilon 1} = 1.5$, $C_{\varepsilon 2} = 1.9$,

$$f_\mu = \left\{1 - \exp\left(\frac{-y^*}{14}\right)\right\}\left[1 + \left(\frac{5}{R_t^{3/4}}\exp\left\{-\left(\frac{R_t}{200}\right)^2\right\}\right)\right], \quad \text{and}$$

$$f_2 = \left[1 - 0.3\exp\left\{-\left(\frac{R_t}{6.5}\right)^2\right\}\right]\left[1 - \exp\left(\frac{-y^*}{3.1}\right)\right]^2.$$

The turbulent Prandtl number, Pr_t, in equation (9) is treated as a function of the distance from the wall, as suggested by Kays and Crawford[44],

$$\mathrm{Pr}_t = \left[\frac{1}{2\mathrm{Pr}_{t\infty}} + \frac{c\mathrm{Pe}_t}{\sqrt{\mathrm{Pr}_{t\infty}}} - (c\mathrm{Pe}_t)^2\left\{1 - \exp\left(\frac{-1}{c\mathrm{Pe}_t\sqrt{\mathrm{Pr}_{t\infty}}}\right)\right\}\right]^{-1} \tag{10}$$

where $\mathrm{Pe}_t = (\mu_t/\mu)\mathrm{Pr}$, $\mathrm{Pe}_{t\infty}$ is the value of Pr_t far from the wall (= 0.8) and c is an empirical constant (= 0.3).

Equations (1)-(5) are discretized with a finite control volume method, employing the QUICK scheme[45] for the convective term in equations (2)-(5). Other terms were discretized by second-order, central differences. In conjunction with the momentum equations, the continuity equation was converted to a pressure correction equation, which was solved via the SIMPLE algorithm[46]. The set of the algebraic equations is solved with Gauss elimination. The convergence criteria of the residuals of all equations was assumed to be less than 10^{-6} of their total inflow rates. The thermal properties are estimated at every iteration by numerical functions described in the following section. The computations were performed on the FUJITSU VPP500 machine.

For the results presented, the numerical grid consisted of eighty nodes with variable spacing between the centerline and the wall, concentrated near the wall. The first node from the wall was located at $y^+ \approx 0.5$ or less. Two thousand nodes with 150 diameters long were employed for predicting the constant properties flow. The nodes in the streamwise direction were distributed uniformly. For comparison to Shehata's experiment, one thousand nodes with sixty diameters long were employed; the last axial node was set at about ten diameters beyond the last useful data point.

Grid dependency was tested by repeating calculations for the "subturbulent" experimental case with 60, 80 and 100 non-uniform nodes in the radial direction. The velocity and temperature profiles at fully-developed region agreed within about one per cent. To investigate the streamwise grid spacing, calculations were conducted with 500, 1000 and 1500 nodes. For all three cases, wall temperature, Nusselt number and pressure drop predictions agreed within one per cent. In addition, predictions with 80 nodes in the radial direction and 1000 nodes in the axial direction were compared to experimental results, as presented in coming sections.

2.2 Thermal Properties

For air, the thermal properties are evaluated as power law functions of the pointwise temperature and pressure with density estimated via the perfect gas approximation[13][47] as follows:

$$\rho = \rho_{ref}\left(\frac{P}{P_{ref}}\right)\left(\frac{T_{ref}}{T}\right) \tag{11}$$

$$\mu = \mu_{ref}\left(\frac{T}{T_{ref}}\right)^{0.67} \tag{12}$$

$$C_p = C_{p,ref}\left(\frac{T}{T_{ref}}\right)^{0.095} \tag{13}$$

$$\lambda = \lambda_{ref}\left(\frac{T}{T_{ref}}\right)^{0.805} \tag{14}$$

The subscript ref indicates that the value was taken at the reference state, typically at the inlet gas temperature and pressure (near 25°C and 0.09 MPa).

2.3 Boundary Conditions

The governing equations are the elliptic sets of partial differential equations. Thus, they require specification of boundary conditions at the entrance, wall and exit along with axi-symmetry. Non-slip, impermeable wall conditions are assumed and the dissipation rate of turbulent energy at the wall is estimated as $\varepsilon_w = 2\nu_w(\partial\sqrt{k}/\partial y)_w^2$, where y represents the coordinate normal to the wall.

The classic case of a fully-developed flow at the thermal entry is approximated as follows. The thermal condition at the wall is taken to be adiabatic for the first twenty five diameters, followed by a specified uniform wall heat flux. Entering conditions are isothermal temperature and approximations of fully-developed mean velocity and turbulence profiles, estimated from the literature in Refs. (44), (48) and (49); these quantities then are allowed to readjust in accordance with the AKN model through the adiabatic entry to yield a new approximation of fully-developed profiles consistent with the model at the start of heating. Outlet conditions are specified by setting streamwise gradients to zero (first partial derivatives for w, u, k, and ε, and the second for T).

3 Predictions of Constant Properties Flows

To validate the numerical code and the turbulence model used in the present study for low-Reynolds-number turbulent flows, we calculated the heat transfer coefficients and friction factors for gas flows in a circular tube with uniform wall heat flux and the constant properties idealization. The flow range was $1900 < \mathrm{Re} < 8000$ and the gas properties were selected for air. For these calculations, the heated region was taken as 125 diameters long, starting at $z/D = 25$. Predicted values of the Nusselt number and friction factor at the outlet are compared to empirical correlations for turbulent flow and to analytical values for laminar flow in Fig. 2; the circles represent the present numerical predictions.

McEligot, Ormand and H. C. Perkins[50] showed that the Dittus-Boelter correlation[9] with the coefficient taken as 0.021 for common gases[26][27][51] is valid within about five per cent for $\mathrm{Pr} \approx 0.7$ and Reynolds numbers greater than about 2500. The present predictions agree closely with it for $\mathrm{Re} > 3200$. Shehata[47] found his measured friction factors for fully-developed turbulent flow to fall between the Blasius relation[48] and the Drew, Koo and McAdams correlation[52]. The agreement with the present friction calculations is also reasonable above $\mathrm{Re} \approx 3200$, ours being about five per cent high. Below this Reynolds number, the predicted Nusselt numbers and friction factors decrease smoothly towards the theoretical laminar values as the Reynolds number decreases, approaching closely for $\mathrm{Re} < 2500$. Below $\mathrm{Re} \approx 2000$, the values for heat transfer differ by about one per cent while friction results differ by about 0.3 per cent.

Torii et al.[32][33] found that their method to predict laminarizing flows coincided with the capability of the fully-established, constant properties calculations to indicate a transition from turbulent to laminar flow near $\mathrm{Re} \approx 2000 - 3000$. The original Nagano and Hishida model[35] lacked this capability as showed in Fig. 2 of Torii et al.[33], where the turbulent prediction was gradually merging to the laminar value as the Reynolds number decreased to about 1000. It is interesting to the present authors that, for flow between parallel plates, the AKN model shows the latter behavior (see Fig. 2a in Abe, Kondoh and Nagano[42]). However, with no change in model constants or functions, the same AKN model can predict reasonable behavior in this sense for a circular tube as in Fig. 2.

As noted in Chapter 2, the present heat transfer predictions are based on the turbulent Prandtl number model recommended by Kays and Crawford (KC). Before choosing this

model, we attempted a "two-equation heat transfer model" and a different Pr_t model. In both cases, predictions for the fully-established Nusselt numbers were about ten per cent or more higher than the Dittus-Boelter correlation, so we selected the KC model as better for our purposes.

In addition to predictions for fully-established flow, it is desirable to determine whether the turbulence model predicts the thermal entry behavior adequately in the Reynolds number range of interest. H. C. Reynolds[53] and Reynolds, Swearingen and McEligot[54] conducted experimental and analytic studies of the thermal entry for low-Reynolds-number flows, providing semi-analytic correlations with the constant property idealization. The local experimental measurements were extrapolated to unity versus T_w/T_b, i.e., constant properties, for comparison (and verification) of the analytic predictions. The experimental uncertainties in the extrapolated Nusselt numbers were estimated to be eight per cent or less for $z/D > 5$. In Fig. 3, predictions from the present model are compared to Reynolds's data at Re = 6800 and 4180. The thermal boundary condition in the experiment was slightly different; at the start of heating, the local heat flux exponentially approached a constant value within a few diameters (also see Shumway and McEligot[55] for a comparable observation for laminar flow). By $z/D \approx 5$, agreement of the predictions presented is good.

In summary, the proposed AKN/KC model appears to perform satisfactorily for constant-properties flow of common gases in pure forced convection in circular tubes.

4 Experiment with High Heat Fluxes

The *experimental objective* of Shehata[40][47] was to measure the distributions of the mean streamwise velocity and temperature for dominant forced convection in a well-defined, axi-symmetric experiment involving significant variation of the gas transport properties across the viscous layer. (This layer – from $y^+ = 0$ to about 30 in adiabatic flow – provides the primary uncertainty in the prediction of thermal and momentum resistances in turbulent wall flows.) Accordingly, experiments were conducted for air flowing upwards in a vertical circular tube heated resistively; the desired distributions were determined via hot wire anemometry.

The *experiment* was conducted in an open loop built around a vertical, resistively-

model, we attempted a "two-equation heat transfer model" and a different Pr_t model. In both cases, predictions for the fully-established Nusselt numbers were about ten per cent or more higher than the Dittus-Boelter correlation, so we selected the KC model as better for our purposes.

In addition to predictions for fully-established flow, it is desirable to determine whether the turbulence model predicts the thermal entry behavior adequately in the Reynolds number range of interest. H. C. Reynolds[53] and Reynolds, Swearingen and McEligot[54] conducted experimental and analytic studies of the thermal entry for low-Reynolds-number flows, providing semi-analytic correlations with the constant property idealization. The local experimental measurements were extrapolated to unity versus T_w/T_b, i.e., constant properties, for comparison (and verification) of the analytic predictions. The experimental uncertainties in the extrapolated Nusselt numbers were estimated to be eight per cent or less for $z/D > 5$. In Fig. 3, predictions from the present model are compared to Reynolds's data at Re = 6800 and 4180. The thermal boundary condition in the experiment was slightly different; at the start of heating, the local heat flux exponentially approached a constant value within a few diameters (also see Shumway and McEligot[55] for a comparable observation for laminar flow). By $z/D \approx 5$, agreement of the predictions presented is good.

In summary, the proposed AKN/KC model appears to perform satisfactorily for constant-properties flow of common gases in pure forced convection in circular tubes.

4 Experiment with High Heat Fluxes

The *experimental objective* of Shehata[40][47] was to measure the distributions of the mean streamwise velocity and temperature for dominant forced convection in a well-defined, axi-symmetric experiment involving significant variation of the gas transport properties across the viscous layer. (This layer – from $y^+ = 0$ to about 30 in adiabatic flow – provides the primary uncertainty in the prediction of thermal and momentum resistances in turbulent wall flows.) Accordingly, experiments were conducted for air flowing upwards in a vertical circular tube heated resistively; the desired distributions were determined via hot wire anemometry.

The *experiment* was conducted in an open loop built around a vertical, resistively-

heated, circular *test section* exhausting directly to the atmosphere in the laboratory. The experiment was designed to approximate a uniform wall heat flux to air, entering with a fully-developed turbulent velocity profile at a uniform temperature. Small single wire probes were introduced through the open exit in order to obtain pointwise temperature and velocity measurements. Details plus tabulations of resulting data are available in a report by Shehata and McEligot[39] with some additional information given by Perkins[13].

A resistively-heated, seamless, extruded Inconel 600 tube of 27.4 mm (1.08 inch) inside diameter was employed as the test section. Heated length between the electrodes was about thirty two diameters and it was preceded by a fifty-diameter, adiabatic entry region for flow development; the short heated length was picked to permit high heating rates with this material while possibly approaching quasi-developed conditions. Outside wall temperatures were determined with premium grade, Chromel Alumel thermocouples distributed along the tube. The axial variation of the static pressure was obtained with pressure taps electrostatically drilled through the wall.

A single *hot wire sensor* was chosen to measure the streamwise velocity and temperature, in preference to an X-probe or other multiple sensor probe, in order to minimize flow disturbances and blockage by prongs and support in the 27 mm tube and to permit measurements closer to the wall. It was employed as a hot wire for velocity measurements and as a resistance thermometer for pointwise temperatures. In addition to the usual difficulties of hot wire anemometry[56], the temperature range of the present experiment introduced additional problems. These difficulties, their solutions and related supporting measurements are described by Shehata[39][47].

Convective and radiative *heat losses* from the outside of the tube were reduced by insulating with a 13 mm (1/2 inch) thick layer of fine silica bubbles, surrounded in turn by electrical heating tapes for guard heating. By this method, heat losses were constrained to less than ten per cent of the thermal energy generation rate except within a few diameters of the electrodes; the heat losses were calibrated so the consequent uncertainties in q''_w were considerably less than the heat loss magnitudes. Heat loss calibration was performed by heating the test section without flow for a range of test section temperatures.

Adiabatic flow runs were conducted for a variety of confidence tests. The flow symmetry was checked by measuring the mean velocity profiles fifty diameters from the plenum chamber for three Reynolds numbers: about 4000, 6000 and 8000. These measurements

were obtained in two perpendicular directions and they coincided, indicating axial symmetry of the flow.

Adiabatic skin friction coefficients were calculated from static pressure differences between a location near the nominal start of heating (z/D defined to be zero) and $z/D \approx$ 19.7 for Reynolds numbers from about 3000 to 10,000. These data fell between accepted correlations for fully-developed turbulent flow: those of Blasius[48] and of Drew, Koo and McAdams[52]. They agreed with the correlations within one to two per cent.

Adiabatic mean velocity profiles were measured for Reynolds numbers of about 4200, 6000 and 8800 at $z/D = 3.17$ using the constant resistance hot-wire anemometer. This location is close enough to the lower electrode so that adiabatic data taken there can serve as measurements of the initial conditions for the heated runs. These data show the same behavior as for fully-developed, low-Reynolds-number pipe flow as measured by Senecal[57], H. C. Reynolds[53] and Patel and Head[58] and predicted by McEligot, Ormand and Perkins[50], H. C. Reynolds[53] and others. As expected, in the turbulent core region, velocities are higher than suggested by the so-called Universal Velocity Profile and this difference is found to decrease as the Reynolds number increases.

Experimental uncertainties were estimated by employing the technique of Kline and McClintock[59], with the sensitivities to the 22 variables involved being deduced by exercising the data reduction program. The uncertainties in pointwise velocity and temperature were most sensitive to the uncertainties in the calibration coefficients and the wire resistance at the gas temperature. The latter was taken as $+/-0.005$ ohm and an uncertainty analysis gave 3.6 and 3.8 per cent for A and B, respectively, in the correlation $\mathrm{Nu} = A + B\mathrm{Re}^n$. The uncertainties in these coefficients were dominated by the uncertainty in the wire diameter which was about two per cent. Examples of the resulting uncertainties in velocity and temperature are tabulated as functions of position and experimental run by Shehata[47].

In general, the uncertainty in velocity was calculated to be in the range of eight to ten per cent of the pointwise value, with the larger percent uncertainties occurring near the wall. The uncertainty in temperature was typically one to two percent of the pointwise absolute temperature. These estimates are believed to be conservative (i.e., pessimistic) since comparisons of the integrated and measured total mass flow rates for each profile showed better agreement – of the order of three per cent or less, except near the exit in the runs with the two highest heating rates (as shown in Table 1). The estimated experimental

uncertainty in the Stanton number was six per cent or less for the range $3 < z/D < 20$ and for the non-dimensional pressure drop it was about four per cent at the last measuring station[13].

Experimental conditions were selected to correspond to three generic situations: 1) essentially turbulent flow with slight, but significant, air property variation, 2) severe air property variation evolving to near laminar flow (as implied by the integral heat transfer parameters) and 3) moderate gas property variation, yielding behavior that could be intermediate or transitional between the first two (and may correspond to "laminarescent" in the terminology of Kline). Perkins[13] and others had found that the thermal development of the third situation was the most difficult of the three to predict. Inlet Reynolds numbers of about 6080, 6050 and 4260 with non-dimensional heating rates, $q^+ = q_w''/Gc_pT_{in}$, of about 0.0018, 0.0035 and 0.0045, respectively, yielded this range. For ease of reference to the reader, these conditions are called Runs 618, 635 and 445. Internal flow data were obtained at five axial locations: 3.17, 8.73, 14.20, 19.87 and 24.54 diameters beyond the lower electrode. Over the range $5 < z/D < 26$ the wall heat flux was uniform to within about three per cent of the average value.

As shown by Torii et al.[33] and Fujii et al.[30], several functions of $q_{in}^+\{\mathrm{Re}_{in}\}$ have been suggested by investigators as criteria for flow regime prediction. Figure 1 presents Shehata's experimental conditions in those terms. One sees that the characterization of his data as turbulent, intermediate and laminarizing is consistent with these criteria.

The length of the test section was chosen to permit measurements through and beyond the normal thermal entry region while attaining significant transport property variation, as exemplified by T_w/T_b and T_w/T_{in}, with common materials and air. Wall temperatures reached 840 K , the maximum wall-to-bulk temperature ratio was about 1.9 and the Mach number was less than 0.013, indicating that compressibility effects would be negligible. On the other hand, at the entrance the buoyancy parameter $\mathrm{Gr}_q/\mathrm{Re}^2$ reached 0.53 for Run445; it then decreased as z/D increased. The maximum wall-to-inlet temperature ratio was about 2.7, indicating that gas properties such as viscosity varied by a factor of two in the test section. Exit bulk Reynolds numbers were above 3000 in all cases, corresponding to turbulent flow if the test section had been adiabatic.

5 Predicted Distributions of Mean Turbulence Quantities

The predicted effects of the model on turbulence quantities of interest are presented in this chapter. The calculations were performed for the conditions of the three experimental runs for which measurements of the mean velocity distributions are available. In these cases, the grid only extended to 35 diameters long beyond the start of the heating. The values of the uniform heat fluxes were chosen to coincide with the average values of $q''_w\{z\}$ in the experiment.

The predicted pointwise values of the *turbulent viscosity* (μ_t/μ) and the behavior of the related turbulent kinetic energy are shown in Fig. 4, where symbols are used to identify axial locations, not data (there were no direct measurements of turbulence quantities); these locations are the same as those where mean velocity and temperature profiles have been measured by Shehata. The abscissae are the normalized wall coordinate; the physical distance from the wall to the centerline. In all three cases, the quantity μ_t/μ is predicted to decrease along the flow first near the wall and then further into the core(Fig. 4(a)). The axial rate at which these phenomena happen increases with q^+. As a measure of an effective viscous layer thickness, y_v, we can choose the location where $(\mu_t/\mu) = 1$. The value y_v/r_w of the inlet profiles for $\mathrm{Re}_{in} \approx 6000$ (Run618 and Run635) is 0.05, and 0.07 in case of $\mathrm{Re}_{in} \approx 4300$ (Run445). By the last measurement station, it is predicted to grow to $y_v/r_w \approx 0.09$, 0.15 and 0.4 for "conditions" 618, 635 and 445, respectively. These predictions are consistent with the earlier suggestion of one of the present authors that the cause of the unexpected reduction in heat transfer parameters could be a thickening of the viscous sublayer (see pp. 131 in Ref. (14)). Between $z/D \approx 3$ and 9, the flattened profile of μ_t/μ in the core disappears as the region affected by the wall grows.

The *turbulent kinetic energy* profiles show some of the same trends (see Fig. 4(b)). Normalization of the turbulent kinetic energy is by a constant, $u^2_{r,in}$, giving a direct measure of the magnitude of the its variation along the tube (i.e., no scaling related to μ, which varies locally with the pointwise temperature). The profiles increase from the wall to a maximum and then decrease to the order of unity at the centerline. An effect of heating appears to be to reduce k near the wall; the higher the heating rate, the greater this effect is calculated to be.

No large changes to the turbulent kinetic energy profiles are forecast for Run618. After

$z/D \approx 9$, the magnitude near the wall only varies slightly; it seems near self-preserving. Further towards the center (about $0.1 < y/r_w < 1$), the variation of the expected profiles is nearly negligible until $z/D > 14$; then the peak increases and values near the centerline decrease as the distance increases. At the last station the peak of $k\{y/r_w\}$ is slightly further from the wall than y_v and is further for Run635 than Run618 — but, in terms of local wall units, this peak remains at $y^+ \approx 14$ for $3 < z/D < 25$. The profiles $k\{y^+\}$ are forecast to remain almost invariant from the wall to $y^+ \approx 10$ while the flow accelerates and the Reynolds number decreases.

For Run635, initially k decreases near the wall and the peak values decrease as well. After $z/D \approx 9$ the rate of change decreases and for the last half of the tube the change is slight, but one could not claim that it appears to become self-preserving. This run might be considered to laminarize near the wall; this effect leads to lower peaks for $3 < z/D < 14$, then the maxima are predicted to become approximately constant but become further from the wall than for Run618, consistent with a physically thicker effective viscous layer. In wall coordinates the variation is less but the trends are the same. With the flow is establishing of the entering profile, the peak value occurs near $y^+ \approx 15$, approximately the same as Run618.

The calculations for Run445 show a significant reduction in turbulence kinetic energy along the tube. A region of low values near the wall grows continuously, giving nearly zero values from the wall to $y/r_w \approx 0.15$ ($y^+ \approx 10$) at the last station. Simultaneously, the peak values decrease continuously and move closer to the center. The centerline value decreases as well but is still non- zero at the last station. These same trends also appear when presented as a function of y^+; no near invariant section is predicted as the profiles continuously decrease in the streamwise direction. Clearly, a laminarization process is being forecast but a hot wire sensor at the centerline would still show turbulent fluctuations[12][19].

It is of interest that the predicted maximum values of the turbulent kinetic energy increase in the downstream direction for Run618 but not for the others. In all cases the flow accelerates in the downstream direction, so the wall shear stress is expected to increase approximately as W_b^2. Consequently, near the wall the gradient $\partial W/\partial y$ would increase so that the production term in the governing equation for turbulent kinetic energy would as well. For Run618 apparently this increase is predicted to be more rapid with respect

to axial distance than the stabilization of the viscous layer due to the acceleration. An alternative explanation could invoke the effects on the dissipation rate. One could calculate the magnitudes of the individual terms as part of the numerical solution and then compare their values to see the predicted relative effects on the local value of the squared-difference-from-the-mean (known as the turbulent kinetic energy), but that exercise is beyond the present intended scope. For Run635 the countering effects at $y^+ \approx 15$ apparently balance so the predicted maxima do not change significantly. Then in Run445 the countering effects near the wall are predicted to be greater than the production term and the profiles of this defined turbulence quantity decrease continuously.

Resulting predictions for turbulent shear stress (Reynolds stress) and *turbulent heat flux* are presented in Fig. 5; these are normalized by local wall values, e.g., $\tau_w\{z\}$. The wall coordinate y^+ is unambiguously defined as $y[g_c\tau_w/r_w]^{1/2}/\nu_w$ with local wall values. These two transport quantities show mostly the same effects as each other except the turbulent heat flux is affected by the growth of the thermal boundary layer at "large" values of y^+.

For Run618 the normalized Reynolds stress profiles are expected to approach a self-preserving condition after $z/D \approx 9$ while the normalized turbulent heat flux appears to be approaching a near asymptotic profile as the thermal boundary layer grows. Predictions for Run635 give lower magnitudes than Run618 for both quantities at equivalent stations. For example, at the last station and $y^+ = 10$ the normalized Reynolds stress profile for Run618 is only slightly lower than the adiabatic entry profile whereas for Run635 the comparable profile is forecast to decrease by about fifty per cent. Peak values are correspondingly lower.

The normalized turbulent heat flux profile, $q_t''\{y^+\}/q_w''$, is predicted to be almost invariant to $y^+ \approx 15$ in Run618. However, for Run635 at $y^+ = 10$, it is expected to decrease by about 2/3 between $z/D \approx 3$ and 25. Peak values of $q_t''\{y^+\}/q_w''$ are predicted to be less for Run635 than for Run618. For both momentum and thermal energy Run635 shows significantly less turbulent transport than Run618, which is considered to be representative of gas flow with property variation that retains its turbulent character. In that sense, Run635 is predicted to be laminarized to some extent; the viscous-dominated region is forecast to become thicker in wall units as well as in physical distance.

Expectations for Run445 are more extreme suppression of turbulent transport than for Run635. The calculations forecast continuous thickening of the viscous-dominated

region and reduction in the maximum values of the normalized Reynolds stresses within the usual viscous layer ($y^+ < 30 - 40$). Beyond $z/D \approx 9$ the same comments hold for the normalized turbulent heat fluxes. The benefits of turbulent transport are predicted to be significantly decreased as the axial distance increases. For example, within 25 diameters the maximum normalized Reynolds stress is expected to decrease to about 0.05, about an order-of-magnitude less than its value for the entering adiabatic profile.

For a slightly higher heating rate ($q^+ \approx 0.0055$), Perkins[13] showed that his "laminar" turbulence model predicted the development of the mean temperature profile well. With his approach, turbulent adiabatic entering profiles were specified and then the governing equations were solved with turbulent viscosity and turbulent thermal conductivity set to zero through the thermal entry region. The present predictions of the development of the turbulent shear stresses and heat fluxes for Run445 demonstrate why Perkins's approach could be successful at higher heating rates; these turbulent transport quantities are forecast to become negligible quickly after the application of the high heating rate.

6 Comparisons to Measurements

Necessary conditions for a turbulence model to be accepted are that it predicts satisfactorily mean velocity and temperature profiles, plus wall heat transfer parameters and pressure drop, for the conditions of interest. The present model is now assessed in those terms. Figure 6 provides direct comparisons of the predictions to measured profiles. The region shown here is selected to emphasize the normal viscous layer with coordinates chosen to avoid the uncertainties involved in the determination of u_τ for non-dimensionalization. For example, for the temperature profiles t_w^+ is represented by $(T_w - T)/T_{in}$. These comparisons of predictions and data are more severe tests than using coordinates based on a wall shear stress which has been fitted in the viscous layer. The measured points nearest the wall correspond to y^+ of about 3 to 5, depending on the heating rate and station. The location $y/r_w = 0.1$ is approximately equivalent to $y^+ \approx 20$ for the entering profiles of Run618 and Run635. At the last station, $y/r_w = 0.5$ is about $y^+ \approx 60$ and 30 for Run618 and Run445, respectively.

The quantity $(T_w - T)/T_{in}$ provides a measure of the gas property variation across the tube. For example, in Run618 $(T_w - T)/T_{in}$ varies by about fifty per cent to $y/r_w = 0.51$

region and reduction in the maximum values of the normalized Reynolds stresses within the usual viscous layer ($y^+ < 30 - 40$). Beyond $z/D \approx 9$ the same comments hold for the normalized turbulent heat fluxes. The benefits of turbulent transport are predicted to be significantly decreased as the axial distance increases. For example, within 25 diameters the maximum normalized Reynolds stress is expected to decrease to about 0.05, about an order-of-magnitude less than its value for the entering adiabatic profile.

For a slightly higher heating rate ($q^+ \approx 0.0055$), Perkins[13] showed that his "laminar" turbulence model predicted the development of the mean temperature profile well. With his approach, turbulent adiabatic entering profiles were specified and then the governing equations were solved with turbulent viscosity and turbulent thermal conductivity set to zero through the thermal entry region. The present predictions of the development of the turbulent shear stresses and heat fluxes for Run445 demonstrate why Perkins's approach could be successful at higher heating rates; these turbulent transport quantities are forecast to become negligible quickly after the application of the high heating rate.

6 Comparisons to Measurements

Necessary conditions for a turbulence model to be accepted are that it predicts satisfactorily mean velocity and temperature profiles, plus wall heat transfer parameters and pressure drop, for the conditions of interest. The present model is now assessed in those terms. Figure 6 provides direct comparisons of the predictions to measured profiles. The region shown here is selected to emphasize the normal viscous layer with coordinates chosen to avoid the uncertainties involved in the determination of u_τ for non-dimensionalization. For example, for the temperature profiles t_w^+ is represented by $(T_w - T)/T_{in}$. These comparisons of predictions and data are more severe tests than using coordinates based on a wall shear stress which has been fitted in the viscous layer. The measured points nearest the wall correspond to y^+ of about 3 to 5, depending on the heating rate and station. The location $y/r_w = 0.1$ is approximately equivalent to $y^+ \approx 20$ for the entering profiles of Run618 and Run635. At the last station, $y/r_w = 0.5$ is about $y^+ \approx 60$ and 30 for Run618 and Run445, respectively.

The quantity $(T_w - T)/T_{in}$ provides a measure of the gas property variation across the tube. For example, in Run618 $(T_w - T)/T_{in}$ varies by about fifty per cent to $y/r_w = 0.51$

at the last station, so μ and k vary by about forty per cent in that region. In contrast, in Run445 they vary by more than that in the first three diameters. At the first station for all runs, the first few velocity data points near the wall appear slightly high relative to appropriate asymptotic behavior, a common feature in experimental measurements (and a good reason not to determine u_τ by fitting $u^+ = y^+$). This location required the longest insertion of the probe support in the experiment so some aspects of the data reduction are more difficult to calculate there.

Overall agreement between the predictions and the measurements is encouraging. Though close examination reveals some differences in detail, the predictions can be considered to be satisfactory at least.

Perkins[13] and Torii et al.[37] found the intermediate conditions most difficult to predict (Run635 here). Run618 shows a slight overprediction of the velocity profile at $z/D \approx 25$ but otherwise all profiles are good. Run445 predictions look good throughout despite having the largest fluid property variation. This result probably occurs because molecular transport increases in importance once the laminarizing process has begun. So if one wishes the most sensitive test of a turbulence model for low-Reynolds-number flows with gas property variation, conditions like those of Run635 may be appropriate.

Since Run635 was recognized in advance as most difficult, two extra sets of internal profiles were measured in the experiment. Agreement between calculations and data is good for the first three stations. Then at $z/D \approx 20$ and 25 the velocity is overpredicted near the wall and at $z/D \approx 25$ the quantity $(T_w - T)/T_{in}$ is overpredicted in the range $0.1 < y/r_w < 0.25$ (corresponding approximately to $8 < y^+ < 20$), i.e., $(T_w - T)/T_{in}$ is underpredicted. In the viscous layer, a higher velocity is caused by a lower value of μ_t, which also leads to a higher thermal resistance in the layer; this higher thermal resistance would interfere with thermal energy transport beyond the region leading, in turn, to lower temperatures further from the heated wall. If one wishes to improve the model further, these observations could provide a starting point. For the present purposes, the level of agreement seen is considered satisfactory.

In thermal designing, predictions of the wall heat transfer parameters and friction are considered to be most important. Figure 7 provides these tests for the present model. Figure 7(a) compares local Stanton numbers; since viscosity increases as the gas is heated, the Reynolds number decreases with an increase in z and the axial progression is from

right to left in the figure. Dashed lines represent asymptotes for fully-established flow of constant property gases (Pr $\approx$ 0.7) as references. High values at the right are the usual high (non-dimensionalized) heat transfer coefficients of the immediate thermal entry; the first data point is at $z/D \approx 0.2$ and the last valid data are at $z/D \approx 25$.

The results are not perfect. But they are within acceptable design accuracy despite the challenging conditions of these flows. The calculations display the trends of the data, e.g., they appear to be laminarizing or not as the case may be. After $z/D \approx 6$ the predictions lie within about eight per cent of the measurements or better. Of the three sets of conditions, calculations for the conditions of Run635 seem best despite being considered the most difficult test. It is probably appropriate here to re-emphasize that the constants and functions in the AKN and KC models have not been readjusted for these calculations.

Wall shear stresses and friction factors are not directly measured in the experiments; pressure differences are. In contrast to fully-developed flows with constant properties, τ_w and C_f cannot be deduced from the raw data without questionable assumptions and approximations, so we compare the predictions to the non-dimensional pressure drops directly. In making these comparisons, one must be careful to use the same definition as employed in the data reduction, specifically $P^+ = \rho_{in} g_c (P_{in} - P)/G^2$ here. For the conditions of these flows, $P^+\{z\}$ provides a test of the combined effects of thermal energy addition, wall friction and vertical elevation change. The relative contributions can be estimated via a local approximation of the one-dimensional momentum equation[60],

$$-\left[2\rho_z g_c D_h (dp/dz)/G^2\right] \approx 8q_z^+ + 4C_{f,z} + 2(\mathrm{Gr}_z^*/\mathrm{Re}_z^2) \qquad (15)$$

with the subscript z representing evaluation at local bulk properties. For Run618 these terms are approximately in the ratios 1:4:3, respectively, so wall friction would account for about half the pressure drop; for Run445, they are about 4:5:5, so friction contributes only about one-third. In the predictions, the turbulence model primarily affects only the friction contribution so it is not surprising that the velocity profiles of Fig. 6 yield the good predictions of Fig. 7(b).

7 Concluding Remarks

The AKN model, developed for forced turbulent flow between parallel plates with the constant property idealization, has been successfully extended to treat strongly-heated gas

right to left in the figure. Dashed lines represent asymptotes for fully-established flow of constant property gases (Pr $\approx$ 0.7) as references. High values at the right are the usual high (non-dimensionalized) heat transfer coefficients of the immediate thermal entry; the first data point is at $z/D \approx 0.2$ and the last valid data are at $z/D \approx 25$.

The results are not perfect. But they are within acceptable design accuracy despite the challenging conditions of these flows. The calculations display the trends of the data, e.g., they appear to be laminarizing or not as the case may be. After $z/D \approx 6$ the predictions lie within about eight per cent of the measurements or better. Of the three sets of conditions, calculations for the conditions of Run635 seem best despite being considered the most difficult test. It is probably appropriate here to re-emphasize that the constants and functions in the AKN and KC models have not been readjusted for these calculations.

Wall shear stresses and friction factors are not directly measured in the experiments; pressure differences are. In contrast to fully-developed flows with constant properties, τ_w and C_f cannot be deduced from the raw data without questionable assumptions and approximations, so we compare the predictions to the non-dimensional pressure drops directly. In making these comparisons, one must be careful to use the same definition as employed in the data reduction, specifically $P^+ = \rho_{in} g_c (P_{in} - P)/G^2$ here. For the conditions of these flows, $P^+\{z\}$ provides a test of the combined effects of thermal energy addition, wall friction and vertical elevation change. The relative contributions can be estimated via a local approximation of the one-dimensional momentum equation[60],

$$-\left[2\rho_z g_c D_h (dp/dz)/G^2\right] \approx 8q_z^+ + 4C_{f,z} + 2(\mathrm{Gr}_z^*/\mathrm{Re}_z^2) \qquad (15)$$

with the subscript z representing evaluation at local bulk properties. For Run618 these terms are approximately in the ratios 1:4:3, respectively, so wall friction would account for about half the pressure drop; for Run445, they are about 4:5:5, so friction contributes only about one-third. In the predictions, the turbulence model primarily affects only the friction contribution so it is not surprising that the velocity profiles of Fig. 6 yield the good predictions of Fig. 7(b).

7 Concluding Remarks

The AKN model, developed for forced turbulent flow between parallel plates with the constant property idealization, has been successfully extended to treat strongly-heated gas

flows at low Reynolds numbers in vertical circular tubes. For thermal energy transport, the KC model was adopted. No constants or functions in these models were readjusted.

Under the idealization of constant fluid properties, predictions for fully-established conditions agreed with the Dittus-Boelter correlation for common gases (coefficient = $0.021^{(51)}$) within about five per cent for Re $>$ 3200. Predicted friction coefficients were about five per cent higher than the Drew, Koo and McAdams[52] correlation in this range. Below Re $\approx$ 2000 both predictions agreed with theoretical laminar values within about one per cent. The local thermal entry behavior, Nu$\{z/D\}$, was further confirmed by comparison to the measurements of H. C. Reynolds[53] for Re $\approx$ 4180 and 6800.

The capability to treat forced turbulent flows with significant gas property variation was assessed via calculations at the conditions of experiments by Shehata[47], ranging from essentially turbulent to laminarizing due to the heating. The apparatus was a vertical circular tube with an unheated entry length for flow development, followed by a resistively heated section which gave an approximately uniform wall heat flux. Inlet Reynolds numbers of about 6080, 6050 and 4260 with non-dimensional heating rates, $q^+ = q''_w/(Gc_pT_{in})$, of about 0.0018, 0.0035 and 0.0045, respectively, were employed as internal mean velocity and temperature distributions were measured by hot wire anemometry.

Predictions forecast the development of turbulent transport quantities, Reynolds stress and turbulent heat flux, as well as turbulent viscosity and turbulent kinetic energy. Results suggest that the run at the lowest heating rate behaves as a typical turbulent flow, but with a reduction in turbulent kinetic energy near the wall. For the highest heating rate all turbulence quantities showed steady declines in the viscous layer as the axial position increased - representative of conditions called laminarizing. For the intermediate run, predictions showed the same trends as the highest heating rate but occurred more gradually with respect to axial distance. These observations are consistent with empirical criteria for these regimes, expressed in terms of $q^+_{in}\{\mathrm{Re}\}$. No direct measurements are available to confirm or refute these distributions; they must be assessed by examination of the mean velocity and temperature distributions that result from these predictions of the turbulent transport quantities.

Overall agreement between the predictions and the measured velocity and temperature profiles is good, establishing confidence in the values of the forecast turbulence quantities – and the model which produced them. Moreover, the model yields predictions

compare well to macroscopic characteristics such as the measured wall heat transfer parameters and the pressure drop. The present numerical procedure could predict the local distributions such as velocity as well as macroscopic characteristics for forced turbulent flows with significant gas property variation and laminarizing flow due to strong heating.

Acknowledgments

The study reported was supported by the Japan Atomic Energy Research Institute (JAERI) and by the Long Term Research Initiative Program of the Idaho National Engineering and Environmental Laboratory / Lockheed Idaho Technologies Company under DOE Idaho Field Office Contract DE-AC07-94ID13223. Mr. Ezato received support as a JAERI Research Scholar and Prof. McEligot as a JAERI Distinguished Foreign Scientist. The experiments of Dr. Shehata were funded by the Office of Naval Research, the National Science Foundation and the University of Arizona. To all we are extremely grateful.

Nomenclature

c_p	: specific heat at constant pressure
C_f	: friction factor,$\tau_w/(\rho_w W_b^2/2)$
$C_{\varepsilon 1}$,$C_{\varepsilon 2}$, C_μ	: constants in turbulence model
D	: diameter; D_h, hydraulic diameter
f_2, f_μ	: functions in turbulence model
G	: mass flux, $(\rho W)_{in}$
Gr^*	: modified Grashof number, gD^3/ν^2
Gr_q	: local Grashof number based on heat flux, $gD^4 q_w''/\nu_b^2 \lambda_b T_b$
g_c	: units conversion factor, e.g., 1 kg m/(N s^2)
g_i	: acceleration of gravity in i-direction
k	: turbulent kinetic energy, $-\overline{u_i u_i}/2$
L	: characteristic turbulence length scales
Nu	: Nusselt number, $\alpha D/\lambda$
P	: mean static pressure
P^+	: non-dimensional pressure drop, $\rho_{in} g_c (P_{in} - P)/G^2$

compare well to macroscopic characteristics such as the measured wall heat transfer parameters and the pressure drop. The present numerical procedure could predict the local distributions such as velocity as well as macroscopic characteristics for forced turbulent flows with significant gas property variation and laminarizing flow due to strong heating.

Acknowledgments

The study reported was supported by the Japan Atomic Energy Research Institute (JAERI) and by the Long Term Research Initiative Program of the Idaho National Engineering and Environmental Laboratory / Lockheed Idaho Technologies Company under DOE Idaho Field Office Contract DE-AC07-94ID13223. Mr. Ezato received support as a JAERI Research Scholar and Prof. McEligot as a JAERI Distinguished Foreign Scientist. The experiments of Dr. Shehata were funded by the Office of Naval Research, the National Science Foundation and the University of Arizona. To all we are extremely grateful.

Nomenclature

c_p	: specific heat at constant pressure
C_f	: friction factor,$\tau_w/(\rho_w W_b^2/2)$
$C_{\varepsilon 1}$,$C_{\varepsilon 2}$, C_μ	: constants in turbulence model
D	: diameter; D_h, hydraulic diameter
f_2, f_μ	: functions in turbulence model
G	: mass flux, $(\rho W)_{in}$
Gr^*	: modified Grashof number, gD^3/ν^2
Gr_q	: local Grashof number based on heat flux, $gD^4 q_w''/\nu_b^2 \lambda_b T_b$
g_c	: units conversion factor, e.g., 1 kg m/(N s^2)
g_i	: acceleration of gravity in i-direction
k	: turbulent kinetic energy, $-\overline{u_i u_i}/2$
L	: characteristic turbulence length scales
Nu	: Nusselt number, $\alpha D/\lambda$
P	: mean static pressure
P^+	: non-dimensional pressure drop, $\rho_{in} g_c (P_{in} - P)/G^2$

compare well to macroscopic characteristics such as the measured wall heat transfer parameters and the pressure drop. The present numerical procedure could predict the local distributions such as velocity as well as macroscopic characteristics for forced turbulent flows with significant gas property variation and laminarizing flow due to strong heating.

Acknowledgments

The study reported was supported by the Japan Atomic Energy Research Institute (JAERI) and by the Long Term Research Initiative Program of the Idaho National Engineering and Environmental Laboratory / Lockheed Idaho Technologies Company under DOE Idaho Field Office Contract DE-AC07-94ID13223. Mr. Ezato received support as a JAERI Research Scholar and Prof. McEligot as a JAERI Distinguished Foreign Scientist. The experiments of Dr. Shehata were funded by the Office of Naval Research, the National Science Foundation and the University of Arizona. To all we are extremely grateful.

Nomenclature

c_p	: specific heat at constant pressure
C_f	: friction factor,$\tau_w/(\rho_w W_b^2/2)$
$C_{\varepsilon 1}$,$C_{\varepsilon 2}$, C_μ	: constants in turbulence model
D	: diameter; D_h, hydraulic diameter
f_2, f_μ	: functions in turbulence model
G	: mass flux, $(\rho W)_{in}$
Gr^*	: modified Grashof number, gD^3/ν^2
Gr_q	: local Grashof number based on heat flux, $gD^4 q_w''/\nu_b^2 \lambda_b T_b$
g_c	: units conversion factor, e.g., 1 kg m/(N s^2)
g_i	: acceleration of gravity in i-direction
k	: turbulent kinetic energy, $-\overline{u_i u_i}/2$
L	: characteristic turbulence length scales
Nu	: Nusselt number, $\alpha D/\lambda$
P	: mean static pressure
P^+	: non-dimensional pressure drop, $\rho_{in} g_c (P_{in} - P)/G^2$

Pe_t : turbulent Peclet number

$\mathrm{Pr}, \mathrm{Pr}_t$: molecular and turbulent Prandtl numbers

q^+ : non-dimensional wall heat flux, q_w''/Gc_pT_{in}

q_t'' : turbulent heat flux, $\rho c_p \overline{ut}$

q_w'' : wall heat flux

r : coordinate in radial direction

r_w : tube radius

Re : Reynolds number, $WD/\nu = GD/\mu$

R_t : turbulent Reynolds number, $k^2/\nu\varepsilon$

St : Stanton number, Nu/(RePr)

T, t : mean temperature and temperature fluctuation

t^+ : non-dimensional temperature, $\rho u_\tau c_p(T_w - T)/q_w''$

U_i, u_i : mean velocity and velocity fluctuation in i-direction

U, u : mean velocity and velocity fluctuation in radial direction

u^+ : non-dimensional velocity, u/u_τ

u_ε : Kolomogorov velocity scale, $(\nu\varepsilon)^{1/4}$

u_τ : friction velocity, $\sqrt{|\tau_w|/\rho}$

W, w : mean velocity and velocity fluctuation in axial direction; also Wilcox dissipation rate

x_i : coordinate in i-direction

y : distance from wall surface

y^+ : non-dimensional distance from wall surface, $u_\tau y/\nu$

y^* : non-dimensional distance from wall surface, $u_\varepsilon y/\nu$

z : coordinate in axial direction

$\overline{(\ )}$: ensemble-average value

$\{\ \}$:function of

Greek symbols

α : heat transfer coefficient, $q_w''/(T_w - T_b)$

δ_{ij} : Kronecker delta

ε : dissipation rate of turbulent kinetic energy, $\nu\overline{(\partial u_i/\partial x_j)(\partial u_i/\partial x_j)}$

λ, λ_t : molecular and turbulent thermal conductivities

μ, μ_t : molecular and turbulent viscosities

ν, ν_t : kinematic viscosity and eddy diffusivities

ρ : density

$\sigma_k, \sigma_\varepsilon$: model constants for turbulent diffusion of k and ε

τ_w : wall shear stress

Subscripts

b : evaluated at bulk temperature

in : evaluated at start of heating

w : evaluated at wall surface

z : evaluated at local axial position

References

(1) Takase, K., Hino, R., and Miyamoto, Y., "Thermal and hydraulic tests of standard fuel rod of HTTR with HENDEL," *J. Atomic Energy Soc. Japan*, **32**-11, 1107 (1990) (in Japanese).

(2) Najmabadi, F., et al., "The ARIES-I Tokamak reactor study. Final Rpt.," UCLA-PPG-1323 (1991), Univ. California, Los Angeles.

(3) Najmabadi, F., et al., "The ARIES-II and ARIES-IV second-stability Tokamak reactors," *Fusion Tech.*, **21**, 1721 (1992).

(4) Wong, C. P. C., Czechowicz, D. G., McQuillan, B. W., Sleicher, R. W., and Cheng, E. T., "Evaluation of U. S. DEMO helium-cooled blanket options," *Symp. Fusion Engrg.*, Champaign, October (1995).

(5) Waganer, L. M., "Innovation leads the way to attractive IFE reactors - Prometheus-L & Prometheus-H," *Proc., IAEA Tech. Comm. Meeting on Fusion Reactor Design and Technology*, UCLA, September (1993).

(6) Yamazaki, S., "Divertor design of SSTR-2," *Proc., Japan-US Workshop on Tokamak Fusion Power Reactors with EC Contribution*, JAERI-memo 04-171, 186 (1992).

(7) Nishio, S., et al., "A concept of DRastically EAsy Maintenance (DREAM) Tokamak reactor," *Proc., IAEA Tech. Comm. Meeting on Fusion Reactor Design and Technology*, UCLA, September (1993).

λ, λ_t : molecular and turbulent thermal conductivities

μ, μ_t : molecular and turbulent viscosities

ν, ν_t : kinematic viscosity and eddy diffusivities

ρ : density

$\sigma_k, \sigma_\varepsilon$: model constants for turbulent diffusion of k and ε

τ_w : wall shear stress

Subscripts

b : evaluated at bulk temperature

in : evaluated at start of heating

w : evaluated at wall surface

z : evaluated at local axial position

References

(1) Takase, K., Hino, R., and Miyamoto, Y., "Thermal and hydraulic tests of standard fuel rod of HTTR with HENDEL," *J. Atomic Energy Soc. Japan*, **32**-11, 1107 (1990) (in Japanese).

(2) Najmabadi, F., et al., "The ARIES-I Tokamak reactor study. Final Rpt.," UCLA-PPG-1323 (1991), Univ. California, Los Angeles.

(3) Najmabadi, F., et al., "The ARIES-II and ARIES-IV second-stability Tokamak reactors," *Fusion Tech.*, **21**, 1721 (1992).

(4) Wong, C. P. C., Czechowicz, D. G., McQuillan, B. W., Sleicher, R. W., and Cheng, E. T., "Evaluation of U. S. DEMO helium-cooled blanket options," *Symp. Fusion Engrg.*, Champaign, October (1995).

(5) Waganer, L. M., "Innovation leads the way to attractive IFE reactors - Prometheus-L & Prometheus-H," *Proc., IAEA Tech. Comm. Meeting on Fusion Reactor Design and Technology*, UCLA, September (1993).

(6) Yamazaki, S., "Divertor design of SSTR-2," *Proc., Japan-US Workshop on Tokamak Fusion Power Reactors with EC Contribution*, JAERI-memo 04-171, 186 (1992).

(7) Nishio, S., et al., "A concept of DRastically EAsy Maintenance (DREAM) Tokamak reactor," *Proc., IAEA Tech. Comm. Meeting on Fusion Reactor Design and Technology*, UCLA, September (1993).

(8) Nishio, S., "DRastically EAsy Maintenance reactor: DREAM-2," *Proc., Japan-US Workshop on Fusion Power Reactors P246*, JAERI-memo 07-100, 160 (1995).

(9) Dittus, F. W., and Boelter, L. M. K., "Heat transfer in automobile radiators of the tubular type," *Pub. in Engrg.* (Univ. California), **2**, 443 (1930).

(10) Iacovides, H., and Launder, B. E., "Computational fluid dynamics applied to internal gas-turbine blade cooling: a review," *Int. J. Heat Fluid Flow*, **16**, 454 (1995).

(11) Mikielewicz, D. P., "Comparative studies of turbulence models under conditions of mixed convection with variable properties in heated vertical tubes," Ph.D. thesis, Univ. Manchester (1994).

(12) Bankston, C. A., "The transition from turbulent to laminar gas flow in a heated pipe," *J. Heat Transfer*, **92**, 569 (1970).

(13) Perkins, K. R., "Turbulence structure in gas flows laminarizing by heating," Ph.D. thesis, Univ. Arizona (1975).

(14) McEligot, D. M., "The effect of large temperature gradients on turbulent flow of gases in the downstream region of tubes," Ph.D. thesis, Stanford Univ. Also TID-19446 (1963).

(15) Coon, C. W., "The transition from the turbulent to the laminar regime for internal convective flow with large property variations," Ph.D. thesis, Univ. Arizona (1968).

(16) Coon, C. W., and Perkins, H. C., "Transition from the turbulent to the laminar regime for internal convective flow with large property variations," *J. Heat Transfer*, **92**, 506 (1970).

(17) McEligot, D. M., Coon, C. W., and Perkins, H. C., "Relaminarization in tubes," *Int. J. Heat Mass Transfer*, **9**, 1151 (1970).

(18) Akino, N., "On the criterion for laminarization in a heated circular tube," *Proc., Fall Meeting, Atomic Energy Soc. Japan*, **A36**, 36 (1978) (in Japanese).

(19) Ogawa, M., Kawamura, H., Takizuka, T., and Akino, N., "Experiment on laminarization of strongly heated gas flow in a vertical circular tube," *J. At. Energy Soc., Japan*, **24**-1, 60 (1982) (in Japanese).

(20) Perkins, H. C., and Worsoe-Schmidt, P. M., "Turbulent heat and momentum transfer for gases in a circular tube at wall-to-bulk temperature ratios to seven," *Int. J. Heat Mass Transfer*, **8**, 1011 (1965).

(21) McEligot, D. M., Magee, P. M. and Leppert, G., "Effect of large temperature gradients on convective heat transfer: The downstream region," *J. Heat Transfer*, **87**, 67(1965).

(22) Petukhov, B. S., Kirillov, V. V., and Maidanik, V. N., "Heat transfer experimental research for turbulent gas flow in pipes at high temperature difference between wall and bulk fluid temperature," *Proc., 3rd Int. Heat Transfer Conf.*, **I**, 285 (1966).

(23) Bankston, C. A., and McEligot, D. M.,"Turbulent and laminar heat transfer to gases with varying properties in the entry region of circular ducts," *Int. J. Heat Mass Transfer*, **13**, 319 (1970).

(24) van Driest, E. R., "On turbulent flow near a wall," *J. Aerospace Sci.*, **23**, 1007 and 1036 (1956).

(25) McEligot, D. M., and Bankston, C. A., "Turbulent predictions for circular tube laminarization by heating," ASME paper 69-HT-52 (1969).

(26) Kawamura, H., "Prediction of heated gas with large property variations using a two-equation model of turbulence," *Trans., JSME*, **B45**-395, 1046 (1979) (in Japanese).

(27) Kawamura, H., "Analysis of laminarization of heated turbulent gas using a two-equation model of turbulence," *Proc., 2nd Intl. Symp. Turb. Shear Flow*, London, 18.16 (1979).

(28) Ogawa, M., and Kawamura, H., "Experimental and analytical studies on friction factor of heated gas flow in circular tube," *J. At. Energy Soc., Japan*, **28-10**, 957 (1986) (in Japanese).

(29) Ogawa, M., and Kawamura, H., "Effects of entrance configuration on pressure loss and heat transfer of transitional gas flow in a circular tube," *Heat Transfer - Japanese Research*, **15**-5, pp. 77(1987).

(30) Fujii, S., "Studies on heat transfer of strongly heated turbulent gas flow in annular ducts," Ph. D. thesis, Univ. Tokyo (1991) (in Japanese).

(31) Fujii, S., Akino, N., Hishida, M., Kawamura, H., and Sanokawa, K., "Experimental and theoretical investigations on heat transfer of strongly heated turbulent gas flow in an annular duct," *JSME International J., Ser. II*, **34**-3, 348(1991).

(32) Torii, S., Shimizu, A., Hasegawa, S., and Higasa, M., "Analysis of the laminarization phenomena in a circular tube by use of a modified k-ε model," *Trans., JSME*, **B55**-518, 3144 (1989) (in Japanese).

(33) Torii, S., Shimizu, A., Hasegawa, S., and Higasa, M., "Laminarization of strongly heated gas flows in a circular tube (Numerical analysis by means of a modified k-ε model)," *JSME International J., Ser. II*, **33**-3, 538 (1990).

(34) Nagano, Y., Hishida, M., and Asano, T., "Improved form of the k-ε model for wall turbulent shear flows," *Trans., JSME*, **B50**-457, 2022 (1984) (in Japanese).

(35) Nagano, Y., and Hishida, M., "Improved form of the k-ε model for wall turbulent shear flows," *J. Fluids Engr.*, **109**, 156 (1987).

(36) Torii, S., Shimizu, A., Hasegawa, S., and Kusama, N., "Laminarization of strongly heated annular gas flows," *JSME International J., Ser. II*, **34**-2, 157 (1991).

(37) Torii, S., Shimizu, A., Hasegawa, S., and Higasa, M., "Numerical analysis of laminarizing circular tube flows by means of a Reynolds stress turbulence model," *Heat Transfer - Japanese Research*, **22**, 154 (1993).

(38) Launder, B. E., and Shima, N., "Second-moment closure for the near-wall sublayer: Development and application," *AIAA Journal*, **27**-10, 1319 (1989).

(39) Shehata, A. M., and McEligot, D. M., "Turbulence structure in the viscous layer of strongly heated gas flows," Tech. report INEL-95/0223, Idaho National Engineering Laboratory (1995).

(40) Shehata, A. M., and McEligot, D. M., "Mean turbulence structure in the viscous layer of strongly-heated internal gas flows. Part I: Measurements, " Submitted to *Int. J. Heat Mass Transfer* (1996).

(41) Abe, K., Nagano, Y., and Kondoh, T., "An improved k-ε model for prediction of turbulent flows with separation and reattachment," *Trans., JSME*, **B58**-554, 57 (1992) (in Japanese).

(42) Abe, K., Kondoh, T., and Nagano, Y., "A new turbulence model for predicting fluid flow and heat transfer in separating and reattaching flows – I. Flow field calculations," *Int. J. Heat Mass Transfer*, **37**, 139(1994).

(43) Nagano, Y., and Tagawa, M., "An improved k-ε model for boundary layer flows," *J. Fluids Engr.*, **112**, 33 (1990).

(44) Kays, W. M., and Crawford, M. E., *Convective heat and mass transfer, 3rd ed.*, New York: McGraw-Hill (1993).

(45) Leonard, B. P., "A stable and accurate convective modeling procedure based on quadratic upstream interpolation," *Comp. Meth. Appl. Mech. and Engrg.*, **19**, 59 (1979).

(46) Patankar, S., *Numerical Heat Transfer and Fluid Flow*, Washington: Hemisphere (1980).

(47) Shehata, A. M., "Mean turbulence structure in strongly heated air flows," Ph.D. thesis, Univ. Arizona (1984).

(48) Schlichting, H., *Boundary layer theory, 6th ed.*, New York: McGraw-Hill (1968).

(49) Hinze, J. O., *Turbulence, 2nd ed.*, New York: McGraw-Hill.

(50) McEligot, D. M., Ormand, L. W., and Perkins, H. C., "Internal low Reynolds number turbulent and transitional gas flow with heat transfer," *J. Heat Transfer*, **88**, 239 (1966).

(51) McAdams, W. H., *Heat transmission, 3rd ed.*, New York: McGraw-Hill, 219 (1954).

(52) Drew, T. B., Koo, E. C., and McAdams, W. M., "The friction factor in clean round pipes," *Trans., A.I.Ch. E.*, **38**, 56 (1932).

(53) Reynolds, H. C., "Internal low-Reynolds-number, turbulent heat transfer," Ph.D. thesis, Univ. Arizona. Also DTIC AD-669-254 (1968).

(54) Reynolds, H. C., Swearingen, T. B., and McEligot, D. M., "Thermal entry for low-Reynolds-number turbulent flow," *J. Basic Engrg.*, **91**, 87 (1969).

(55) Shumway, R. W., and McEligot, D. M., "Laminar gas flow in annuli with property variation," *Nuc. Sci. Eng.*, **46**, 394 (1971).

(56) Sandborn, V. A., *Resistance temperature transducers*, Fort Collins, Colo.: Metrology Press (1972).

(57) Senecal, V. E., "Fluid flow in the transition zone," ScD thesis, Carnegie Institute of Technology (1951).

(58) Patel, V. C., and Head, M. R., "Some observations on skin friction and velocity profiles in fully developed pipe and channel flows," *Fluid Mech.*, **36**, 181 (1969).

(59) Kline, S. J., and McClintock, F. A., "Describing uncertainties in single-sample experiments," *Mech. Engr.*, **75**-1, 3 (1953).

(60) McEligot, D. M., Smith, S. B., and Bankston, C. A., "Quasi-developed turbulent pipe flow with heat transfer," *J. Heat Transfer*, **92**, 641 (1970).

Table 1. Discrepacy between integrated mass flux (velocity) profiles and measureed mass flow rates in the experiment.

Run	q_{in}^{+}	Re_{in}	$z/D = 3.17$	8.73	14.20	19.87	24.54
618	0.0018	6080	0.015	—	0.032	—	0.027
635	0.0035	6050	0.027	0.001	0.037	0.022	0.061
445	0.045	4260	0.017	—	0.012	—	0.071

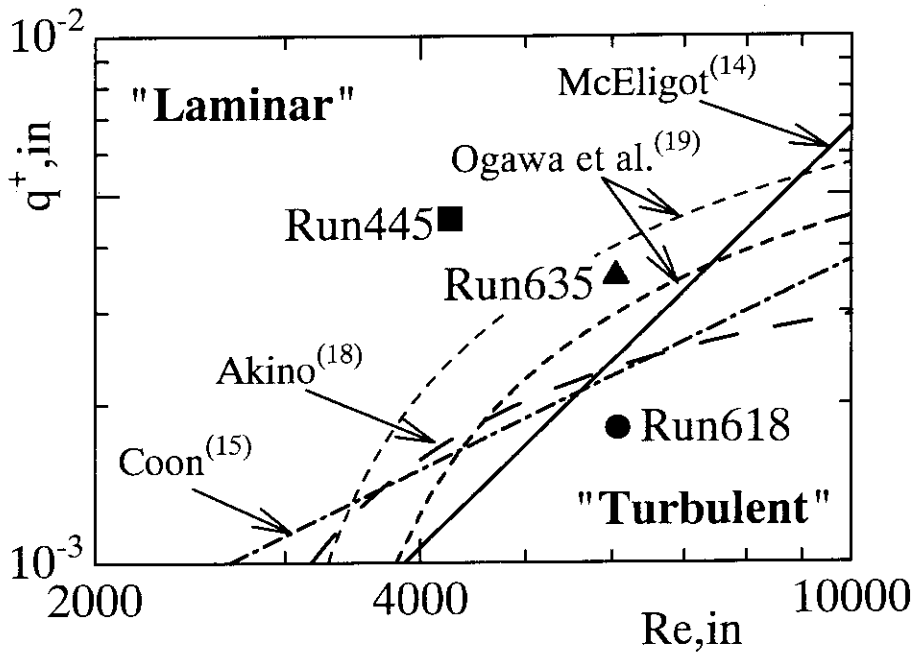

Figure 1. Proposed criteria for laminarization of heated gas flow in circular tubes with approximately constant heat flux [Fujii[30]]; symbols = conditions of experiments by Shehata[47].

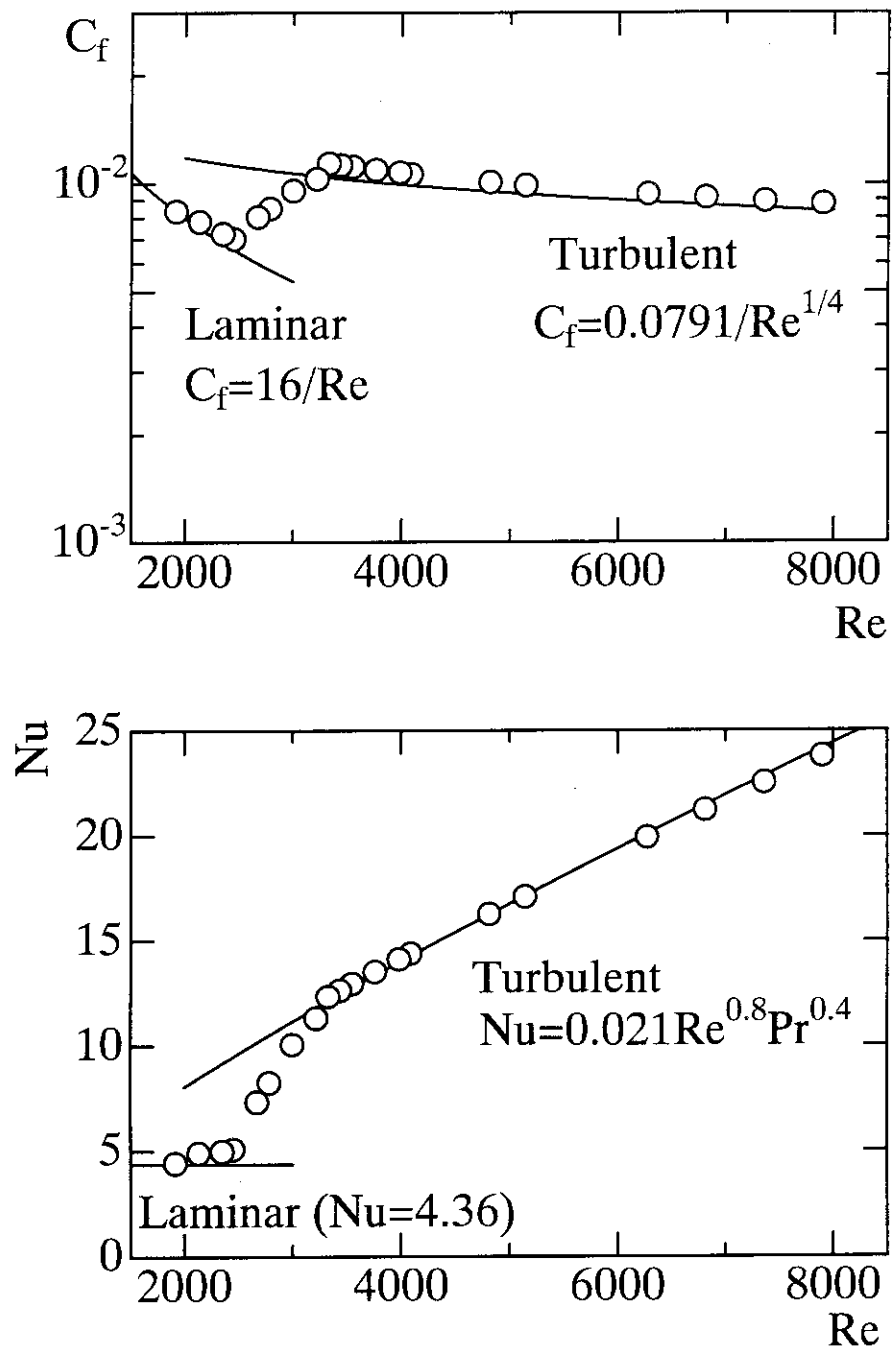

Figure 2. Comparison of predictions from present model (circles) to empirical turbulent correlation's and theoretical laminar results for fully-established flow with constant fluid properties.

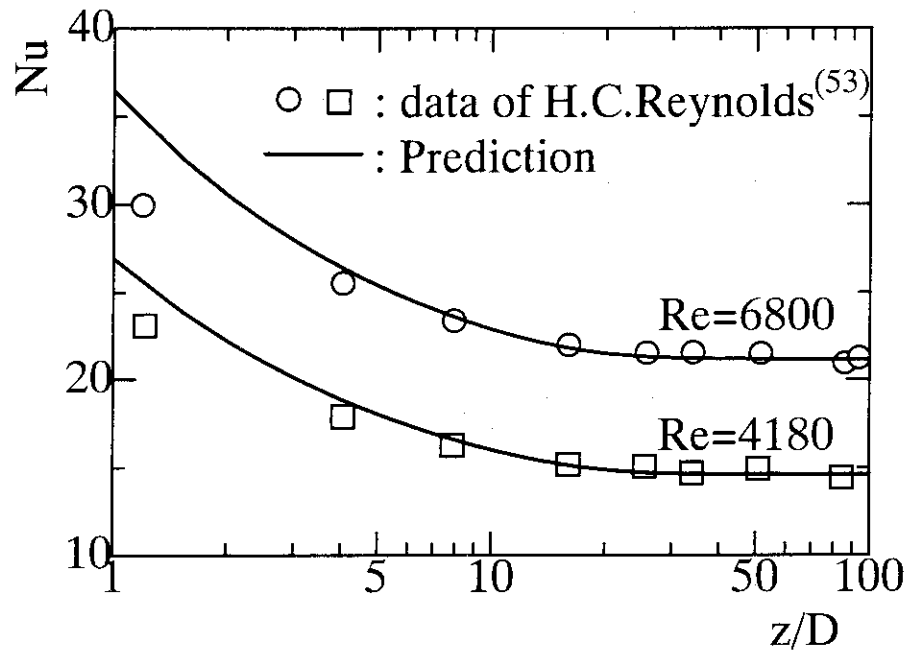

Figure 3. Comparison of predictions from present model to thermal entry measurements of H. C. Reynolds[53], constant fluid properties.

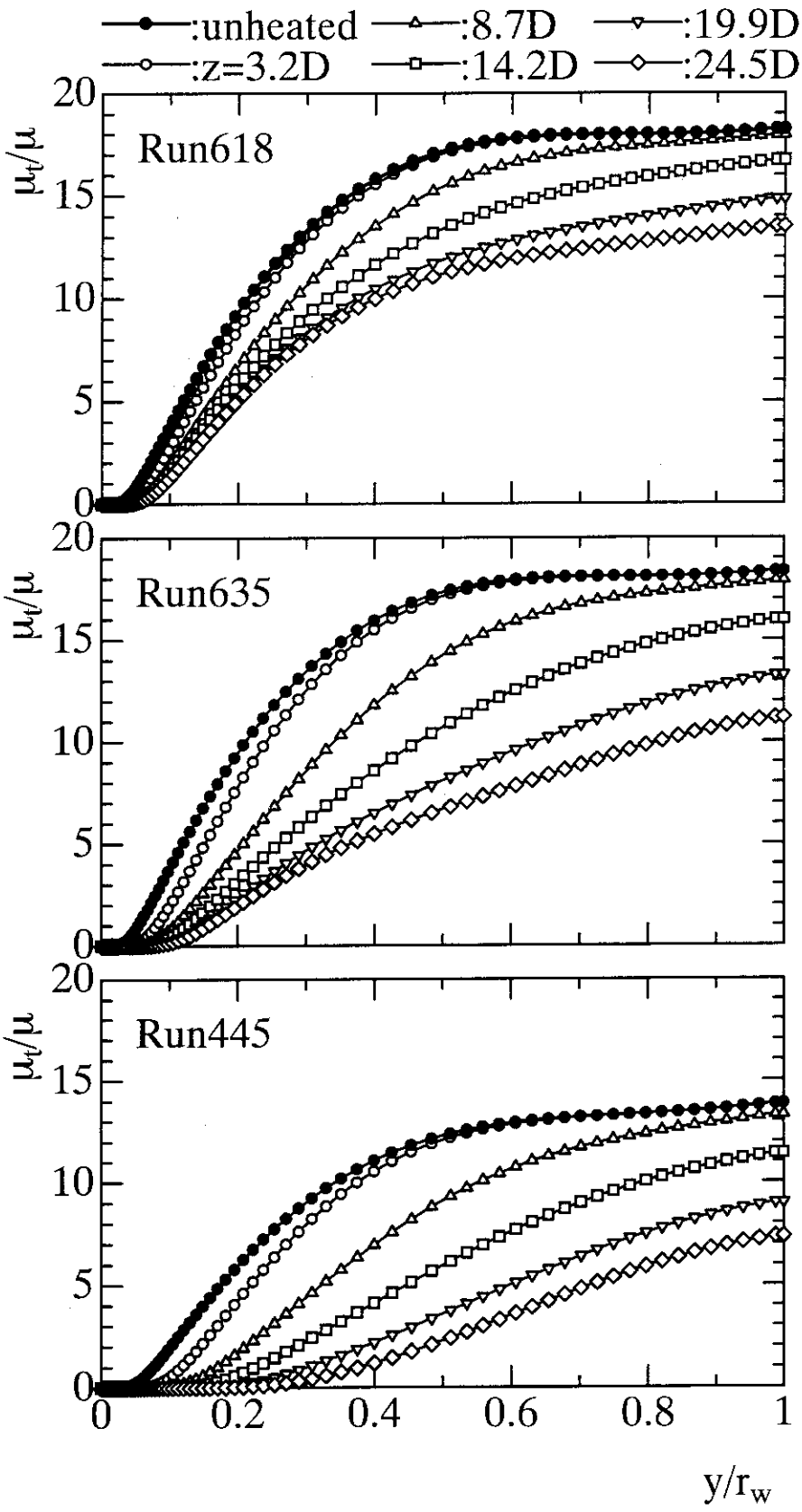

Figure 4(a). Predicted axial development of turbulent quantities for conditions of experiments by Shehata[47]: (a) turbulent viscosity.

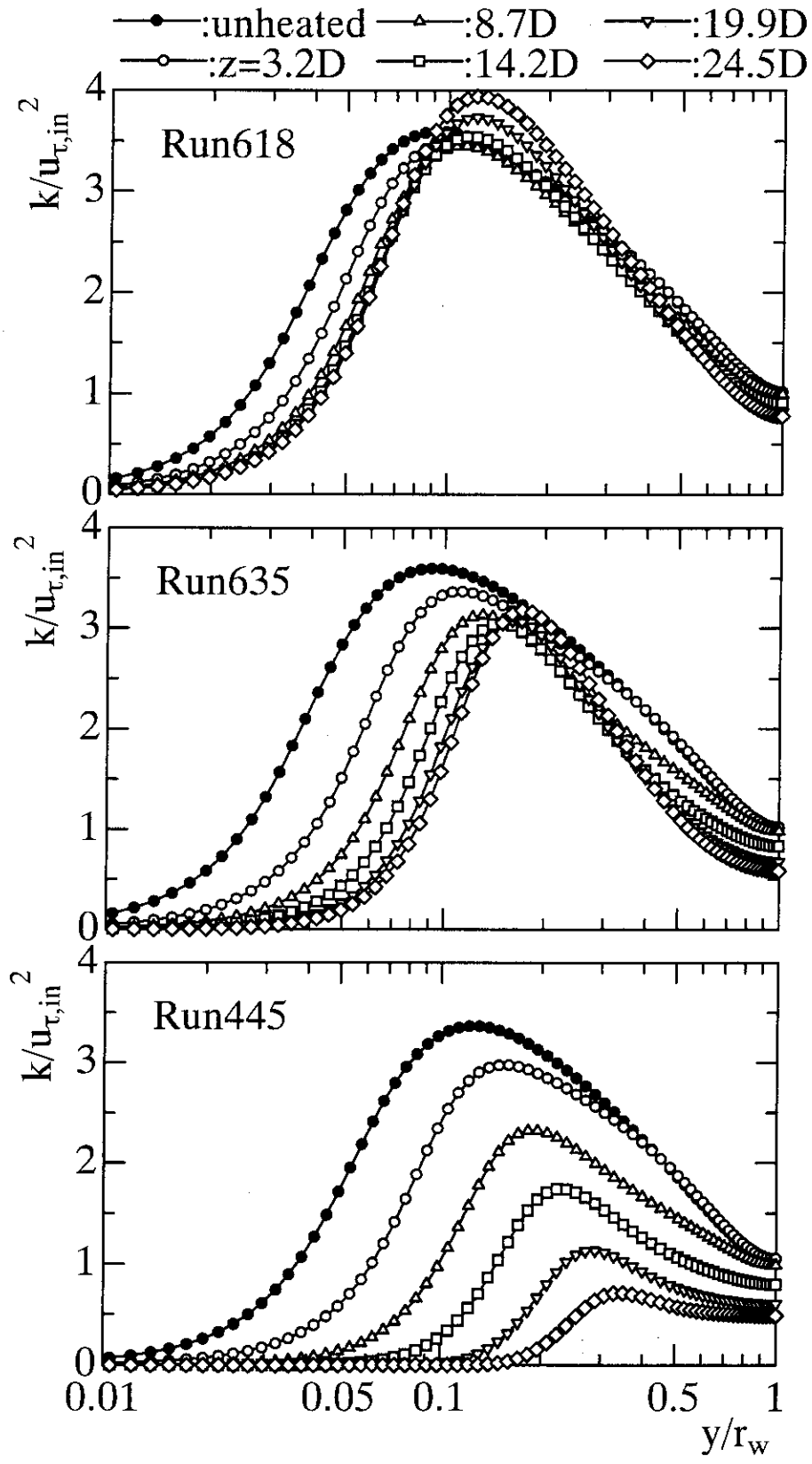

Figure 4(b). Predicted axial development of turbulent quantities for conditions of experiments by Shehata[47]: (b) turbulent kinetic energy.

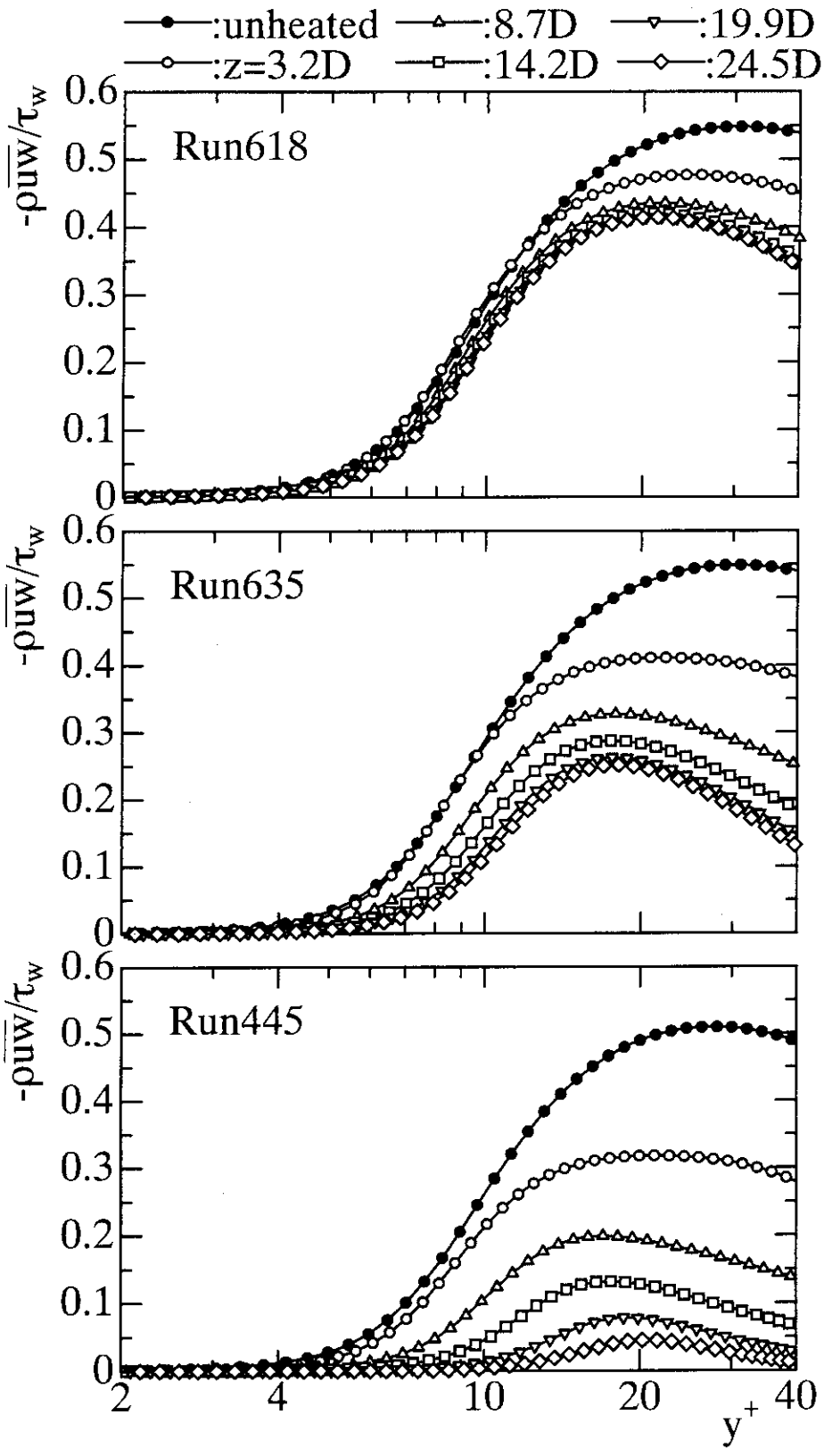

Figure 5(a). Predicted axial development of turbulent transport quantities for conditions of experiments by Shehata[47]: (a) Reynolds stress.

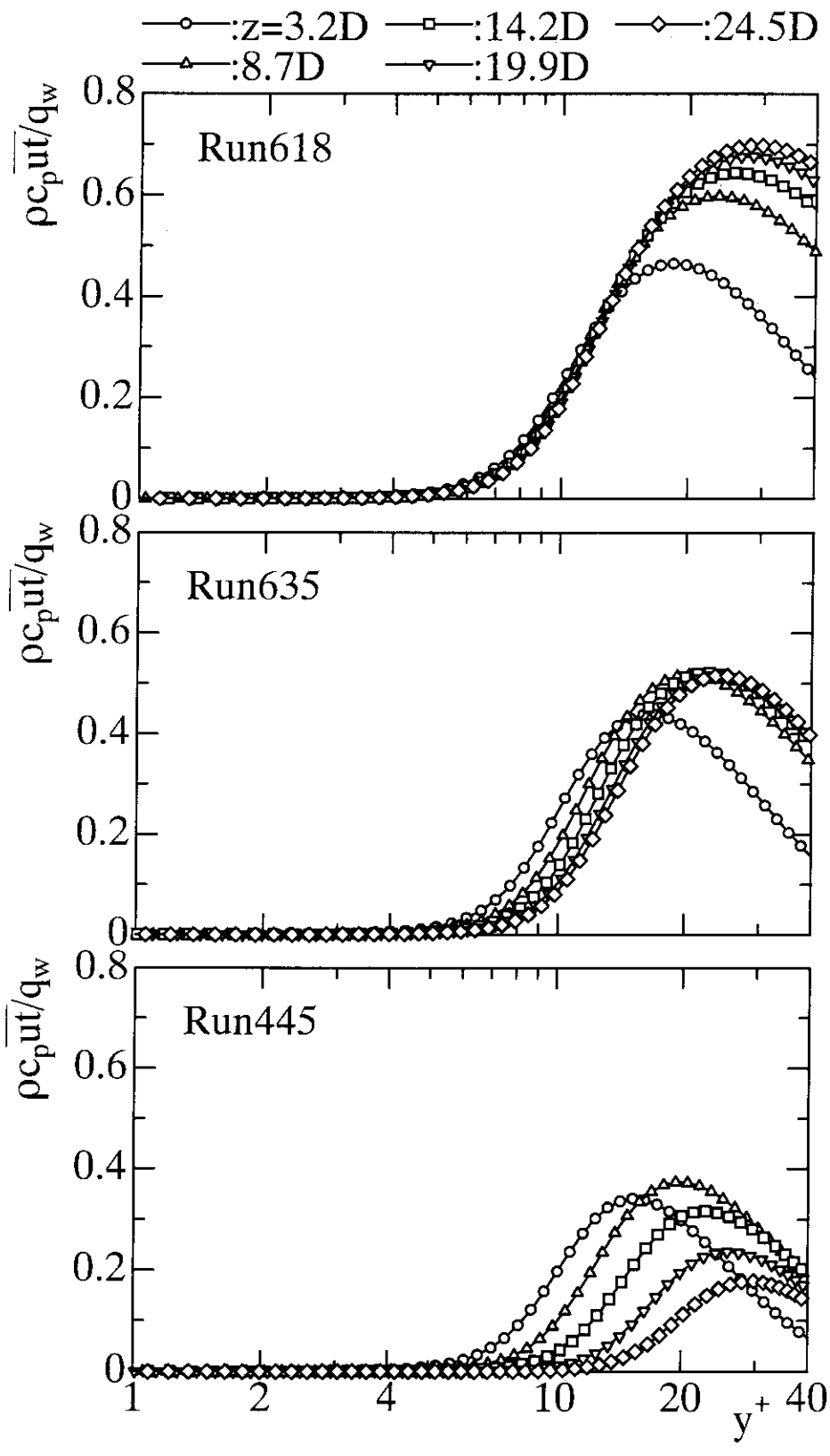

Figure 5(b). Predicted axial development of turbulent transport quantities for conditions of experiments by Shehata[47]: (b) turbulent heat flux.

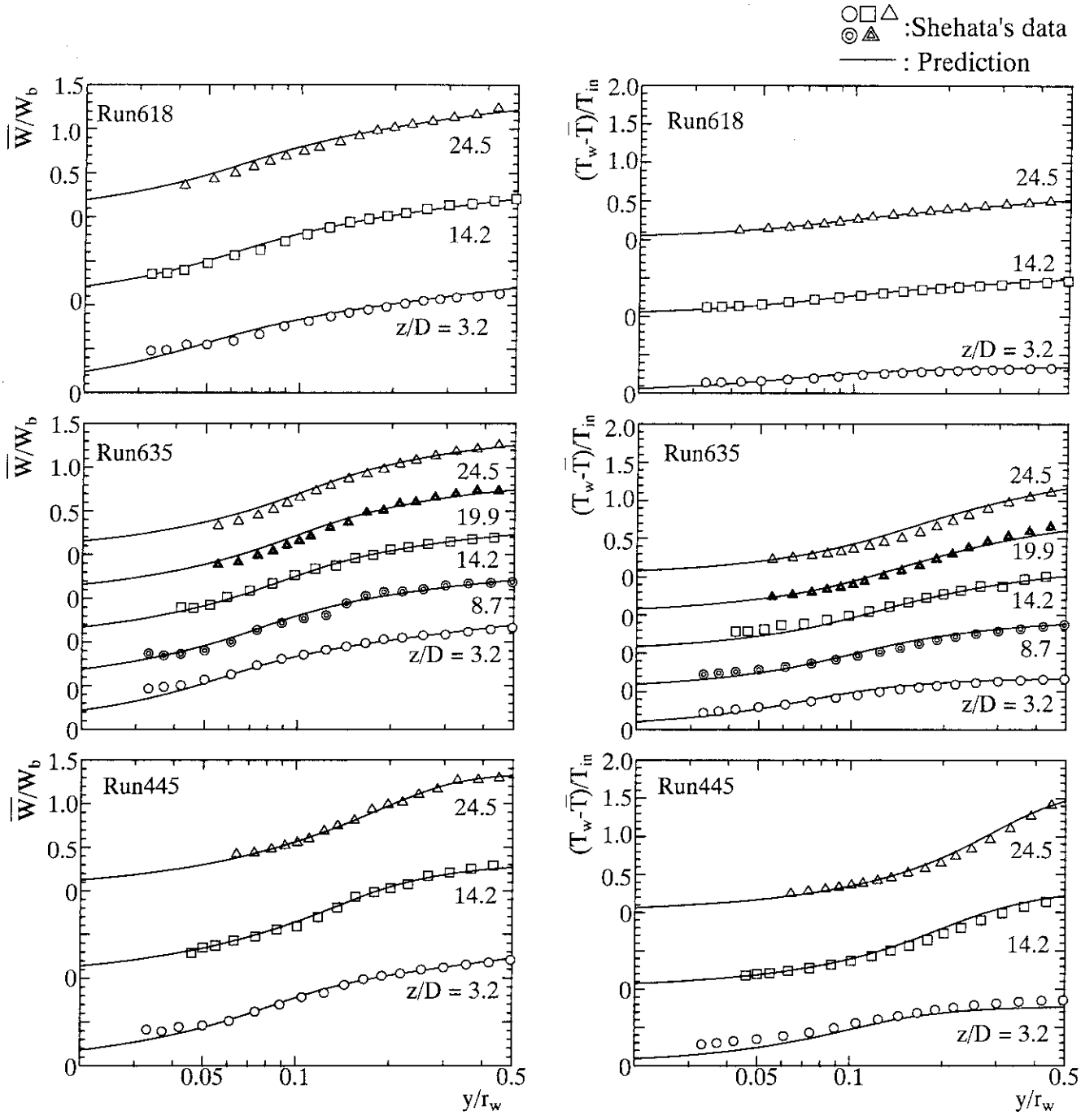

Figure 6. Predicted axial development of mean streamwise velocity and mean temperature (solid lines) compared to measurements (symbols) of Shehata[47] with strong heating of air in a vertical circular tube.

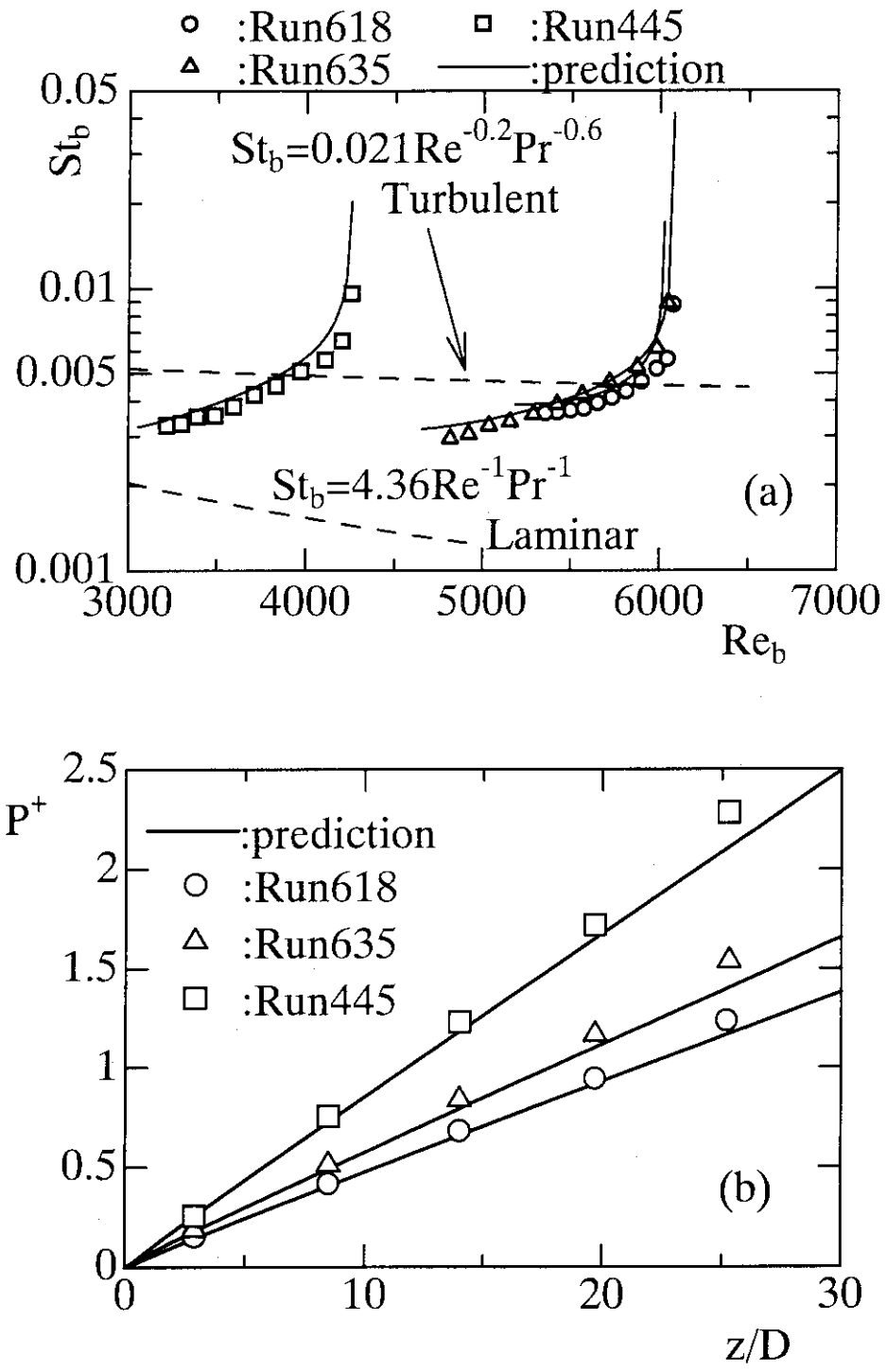

Figure 7. Predicted local integral parameters (solid lines) compared to measurements (symbols) of Shehata[47]: (a) wall heat transfer and (b)non-dimensional pressure drop.